NOAA Technical Memorandum NOS CS 55

VDatum Update for Chesapeake Bay, Delaware Bay, and Adjacent Waters: Tidal Datums, Sea Surface Topography, and Their Spatially Varying Uncertainties

Silver Spring, Maryland
April 2023

noaa National Oceanic and Atmospheric Administration

U.S. DEPARTMENT OF COMMERCE
National Ocean Service
Coast Survey Development Laboratory

Office of Coast
Survey National
Ocean Service
National Oceanic and Atmospheric
Administration
U.S. Department of Commerce

The Office of Coast Survey (OCS) is the Nation's only official chartmaker. As the oldest United States scientific organization, dating from 1807, this office has a long history. Today it promotes safe navigation by managing the National Oceanic and Atmospheric Administration's (NOAA) nautical chart and oceanographic data collection and information programs.

There are four components of OCS:

The Coast Survey Development Laboratory develops new and efficient techniques to accomplish Coast Survey missions and to produce new and improved products and services for the maritime community and other coastal users.

The Marine Chart Division acquires marine navigational data to construct and maintain nautical charts, Coast Pilots, and related marine products for the United States.

The Hydrographic Surveys Division directs programs for ship and shore-based hydrographic survey units and conducts general hydrographic survey operations.

The Navigational Services Division is the focal point for Coast Survey customer service activities, concentrating predominately on charting issues, fast-response hydrographic surveys, and Coast Pilot updates.

NOAA Technical Memorandum NOS CS 55

VDatum Update for Chesapeake Bay, Delaware Bay, and Adjacent Waters: Tidal Datums, Sea Surface Topography, and Their Spatially Varying Uncertainties

Elena Tolkova[1,2], Liujuan Tang[2], Jack Riley[2], Inseong Jeong[3,4], Stephen White[4]

1. Earth Resources Technology, Inc., Laurel, MD
2. Office of Coast Survey, Coast Survey Development Laboratory, Silver Spring, MD
3. University Corporation for Atmospheric Research, Boulder, CO
4. National Geodetic Survey, Remote Sensing Division, Silver Spring, MD

April 2023

noaa National Oceanic and Atmospheric Administration

U. S. DEPARTMENT OF COMMERCE
Gina Raimondo, Secretary

National Oceanic and Atmospheric Administration
Richard Spinrad, Under Secretary

National Ocean Service
Nicole LeBoeuf, Assistant Administrator

Office of Coast Survey
Rear Admiral Benjamin Evans
Director

Coast Survey Development Laboratory
Corey Allen
Acting Division Chief

NOTICE

Mention of a commercial company or product does not constitute an endorsement by NOAA. Use for publicity or advertising purposes of information from this publication concerning proprietary products or the tests of such products is not authorized.

TABLE OF CONTENTS

LIST OF FIGURES

LIST OF TABLES

OVERVIEW

This work describes calculation of a revised set of tidal datums[1] for Chesapeake Bay, Delaware Bay, and adjacent coastal waters, to be used with the NOAA's vertical datum transformation software tool, VDatum. The original set of tidal datums for the area was developed in 2008 (Yang et al., 2008). The purpose of the revision was to re-calculate datums based on the updated observational data set on 1983-2001 EPOCH[2], and extrapolate the datums up to 500 m inland. Datum calculation is comprised of the next steps:

- *modeling:* hydrodynamic modeling of tides in the area with a 2D barotropic hydrodynamic model, ADCIRC; model parameters to be adjusted in trial runs for a better match between tidal datums calculated with modeled time histories and tidal datums observed at water level stations;

- *assimilation of observations:* model datum errors at stations locations - discrepancies between model results and datums derived from observations - were interpolated over the model domain to obtain a correction field for each of the tidal datums;

- *population of marine grids:* corrected datums are interpolated onto a set of structured rectangular grids and extended at least 500 m inland from the coastline.

For the modeling step, this revision uses the same computational grid - an unstructured triangular-element grid consisting of 318,860 nodes and 558,718 cells - developed for the 2008 model. The model was forced with 13 tidal harmonic constituents extracted from the improved Western North Atlantic ADCIRC Tidal Database (Szpilka et al., 2015). Observational set used to adjust model parameters and validate the results was different from the observational set used in 2008. Tidal datums were calculated directly from the modeled water level time histories three nodal cycles (44.5 days) in duration, using in-house *lv8j* software that emulates CO-OPS datum calculation algorithm. This is different from the datum calculation approach employed in 2008. For the 2008 model, modeled time histories were, first, subjected to harmonic analysis for 37 tidal constituents; then the resulting constituents were used to synthesize water level time series over the entire Nation Tidal Datum Epoch (1983-2001), and finally, tidal datums were computed from those 19-year long time histories.

Assimilation of observations was based on a method suggested by (Shi and Myers, 2016) which applies statistical interpolation to the model datum errors. Differently, the 2008 datum

[1] A tidal datum is a standard elevation defined by a certain phase of the tide: https://tidesandcurrents.noaa.gov/datum_options.html

[2] An epoch is a 19-year tidal cycle used to calculate datums

calculation was based on the tidal constituent and residual interpolation (TCARI) method for deriving a correction field for each modeled datum (Hess, 2002, 2003).

Marine grids were re-developed to increase resolution and allow for extended VDatum coverage. The above steps of the datum calculation procedure are detailed further.

1. DATA

1.1. Bathymetry

With a single insignificant modification described in section 3.5, the computational bathymetric grid used for the modeling is the one developed and used in the 2008 version of the model. Please see (Yang et al., 2008) for bathymetric sources, as well as description of land features included in the model.

1.2. Water level data

NOAA's Center for Operational Oceanographic Products and Services (CO-OPS) computes tidal datums using water level time histories available from their National Water Level Observation Network (NWLON). In the VDatum program, these observed tidal datums at water level stations (aka tidal gages) in the model domain are used for both model validation and calculation of the final areal datums (Milbert and Hess, 2001; Shi and Myers, 2016). Thus availability and the spatial distribution of water stations greatly affect the accuracy of the modeling and the final results, as well as the inland extent of VDatum regions which generally extend up to or shortly past the farthest inland water level station.

The current model and the 2008 model use different ensembles of tidal gages. The 2008 model used 298 gages, while the current model was validated with 129 gages, of which 108 gages were also used in 2008, and 21 gages were newly added. Thus, 190 gages used in 2008 are not used in the updated version. Five of the latter stations seem to be replaced with the new ones with different IDs, but practically in the same locations. Figure 1 shows locations of the old gages carried over into the updated version (violet circles), the newly added gages used by the updated version (blue and red circles), and the old gages not used here (green); as well as updated bounding polygons (see section 5.1 for the BPs). Red circles represent seven gages (four of which on the model's south are visually coincide and covered by a violet circle) which do not reside within the computational domain (and therefore could not be used for the model validation), but fall within or near respective marine grids and were used at the data assimilation step.

The reason for excluding a large number of stations was that these stations had datums not on the current EPOCH and did not meet the CO-OPS quality requirements, such as: there may have been less than 30 days of data, there were no bracketing levels, there was missing metadata. Only datums on the 1983-2001 EPOCH were included in the complete list that CO-OPS delivered for the use with the present development (Michael Michalski, personal communications).
The 136 stations used for calculation of the updated datums, with their IDs, location, and observed datums relative to local MSL are listed in Table 11, Appendix A.

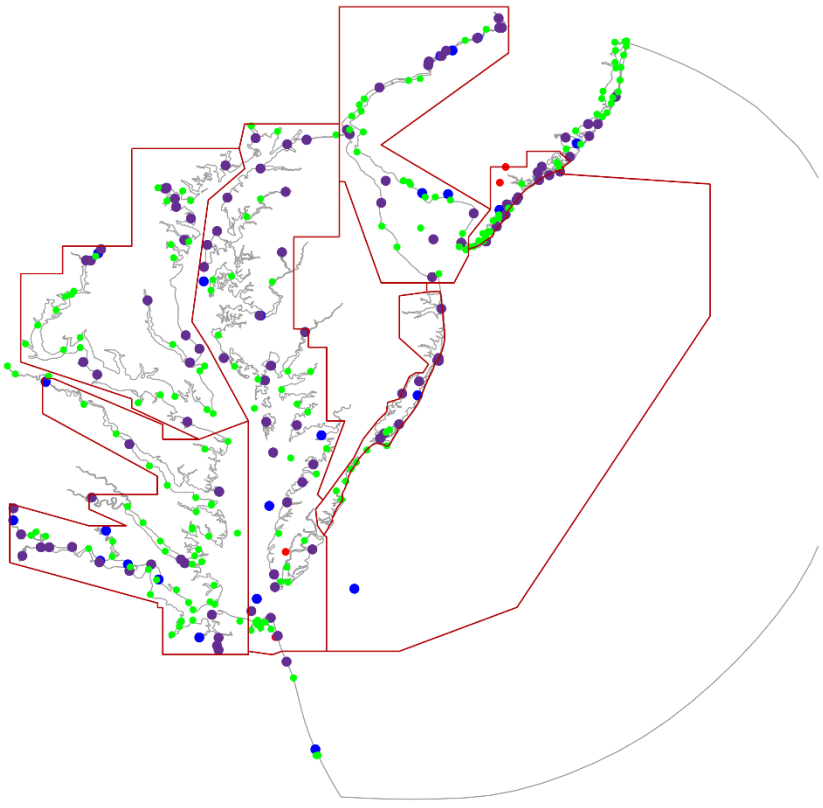

Figure 1. *violet circles:* tidal gages used by the 2008 model and carried over into the updated version; *blue:* newly added gages used to verify the updated version; *green:* tidal gages used by the 2008 model and not used presently; *red:* gages outside the computational domain, but within or near respective marine grids; *dark red line:* updated bounding polygons, see also Figure 21.

2. MODEL SET-UP

2.1. Model grid

The model domain extends from New Jersey on the North to Virginia on the South, and extends landward to include large rivers emptying into Chesapeake Bay: Patuxent, Potomac, Rappahannock, York, and James rivers. It covers Delaware Bay and lower Delaware River, Chesapeake Bay, embayments along New Jersey (NJ), Delaware (DE), Maryland (MD), and Virginia (VA) coasts, and adjacent coastal waters. The model domain is represented by a high-resolution, unstructured grid developed in 2008. The grid consists of 318,860 nodes and 558,718 triangular elements, with spacing ranging from around 13 m in shallow inland basins to 19 km in deep waters offshore (Yang et al., 2008).

2.2. Hydrodynamic model

Modeling was performed with the ADvanced CIRCulation (ADCIRC) model (Westerink et al., 1993), in a 2-dimensional mode. The model solves depth-averaged shallow-water equations on an unstructured grid, and is widely used for modeling tides in multi-scale environments from open ocean to river channels. Tidal forcing on the ocean boundary was applied. Tidal motion was simulated for 54.5 days with a 1.8 s time increment. The first 10 days of simulation were used to establish the tidal motion in the domain. Water level time series for the following 44.5 days (three nodal cycles) were recorded with a 6-min interval, for the datum calculation.

2.3. Boundary forcing: tides and riverine flow

Three boundary types are used in the model:
ocean boundary (50 nodes) where tidal elevation is prescribed;
land boundary where zero normal flow is prescribed; and
river inflow boundary where normal inflow due to freshwater discharge is prescribed.
The river inflow was applied only across a 6-node wide upper boundary of the Delaware river, where 2 m^2/s vertically integrated flux (which in 7-8 m depth, corresponds to 0.3 m/s flow speed) was prescribed. Note that ADCIRC river inflow boundary does not provide adequate representation of a tidal river environment unless the domain extends past the tidal reach, since this condition allows the river flow in, but does not allow the tide to radiate out. The tidal wave loses all its kinetic energy at the upriver boundary, which results in artificially increased tidal ranges and, consequently, the datums. To offset this effect, upriver friction was set higher than it might be in the real world.

On the ocean boundary, the model was forced with 13 Harmonic Constituents (HC) - M2, N2, S2, K1, O1, K2, Q1, P1, M4, L2, M6, MN4, MS4. The constituents' amplitudes and phases relative to the equilibrium tide were extracted from the improved ADCIRC tidal database for Western North Atlantic (Szpilka et al., 2015). The selected constituents are those which had an

amplitude over 1 cm at any point on the ocean boundary. Following the original model of the 2008, the constituents' nodal factors were set to 1 and all equilibrium arguments were set to 0.

2.4. Friction

Acceleration term due to bottom stress in the vertically-integrated momentum equation in ADCIRC-2DDI has a form:

$$\frac{\vec{\tau}}{\rho \cdot h} = -\frac{C_d \cdot u \cdot \vec{u}}{h}$$

where $\vec{\tau}$ is the bottom stress, ρ is the water density, h is the hight of the water column from the bottom to the surface, $\vec{u}$ is the fluid particle velocity with the magnitude u, and C_d is the drag coefficient (Luettich and Westerink, 2004). ADCIRC also allows for the Manning friction formulation implemented by re-calculating an effective drag coefficient for each node at every time step as

$$C_d = \frac{gn^2}{h^{(1/3)}},$$

where g is the gravitational acceleration, and n is the Manning's roughness coefficient; C_d is limited from below by its minimal value specified in the input parameter file (0.0025 in our case).

This version of the model uses Manning friction formulation with spatially-varying bottom roughness - different from the 2008 version where quadratic friction scheme with spatially-varying drag coefficient was employed. The bottom roughness was adjusted in multiple trials aiming to minimize model-data discrepancies in the tidal datums. Figure 2 displays the resulting Manning roughness coefficient. The latter varies from 0.015 $s/m^{1/3}$ offshore to 0.043 $s/m^{1/3}$ in some inland basin, which is an expected, physically sound spatial pattern for the Manning roughness coefficient.

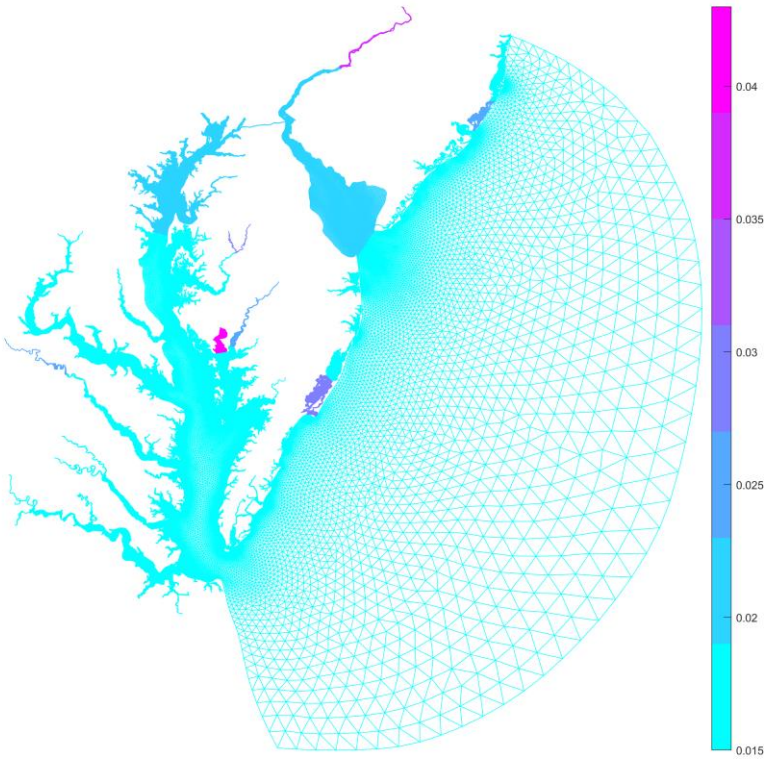

Figure 2. Manning bottom roughness coefficient, color scale: s/m^(1⁄3)

2.5. Bathymetry modification from the previous model

The current model update uses the same numerical grid as the original 2008 model, except for depth modification (deepening) in a waterway from Tolchester Bay, MD to Chesapeake City, MD. This modification was meant to improve the agreement between modeled and observed tidal datums at Chesapeake City. The city is located on the banks of a 14-mile-long, 450-foot-wide and 35-foot-deep ship canal that connects the Delaware River with the Chesapeake Bay in the states of Delaware and Maryland. One would expect that tidal level anywhere in the canal is determined by tidal levels at its opening into the Chesapeake Bay and the Delaware River, likely being a weighted average of the levels at the openings with the weights depending on the location inside the canal. Consequently, one would also expect that good agreement between the model and the observations near the both canal entrances warrants the good agreement everywhere inside the canal.

There are several water stations near the both entrances used for the model validation, as shown in Figure 3. It was fairly straightforward to match observed datums at these stations by adjusting friction in the respective basins while using the original grid. However, in spite of good match just outside the canal entrances, tidal levels at the Chesapeake City had been significantly overestimated by the model - see Figure 4. All attempts to reduce tidal signal in the canal by increasing friction had failed, as the tidal signal had remained practically the same in a wide range of attempted Manning roughness coefficients (0.02 to 0.06) in the canal - supportive of the assertion that this signal is prescribed by tides at the canal entrances.

A simulation with a realistic tidal forcing - nodal factors and arguments were selected for 01/01/2020 to 02/28/2020 - was used to investigate the reliability of the modeling. Stations closest to Chesapeake City, which were active at this time window, are the stations at Reedy Point, DE and Tolchester Bay, MD, circled in Figure 3. Modeled tides vs observed tides at the three locations - Tolchester Bay, Chesapeake City, and Reedy Point - are shown in Figures 5 - 7. The model indeed reproduced the observations (excluding non-tidal variance) outside the canal entrances reasonably well, but greatly overestimated tides at Chesapeake City.

Furthermore, Figures 8 and 9 display tidal signals at all three gages in the same axes, observed and modeled, respectively. Next, we attempted to approximate water levels at Chesapeake City with a linear combination of water levels at the other two gages. Indeed, gage readings at Tolchester Bay and Reedy Point, combined with weights 0.48 and 0.52 respectively for the observed time histories, and with weights 0.23 and 0.77 for the modeled time histories, provide a close approximation to a respective time history at Chesapeake City (see Figures 8 and 9). The conclusion from this experiment is that the model incorrectly admits in the canal much more tidal influence from the east than from the west.

To repair the issue, the bathymetry was modified west of Chesapeake City, as shown in Figure 10. Inside the canal, all depths west of Chesapeake City shallower than 10 m (33 ft) were set to 10 m; while in an adjacent 17-km-long segment of the waterway in the Chesapeake Bay, all depths shallower than 7 m were set to 7 m. This change has saved the model’s quality in the canal while having no effect on tidal heights at other locations. Substantially improved agreements between modeled and observed tidal signals and tidal datums are seen in Figure 11 and Figure 12, respectively.

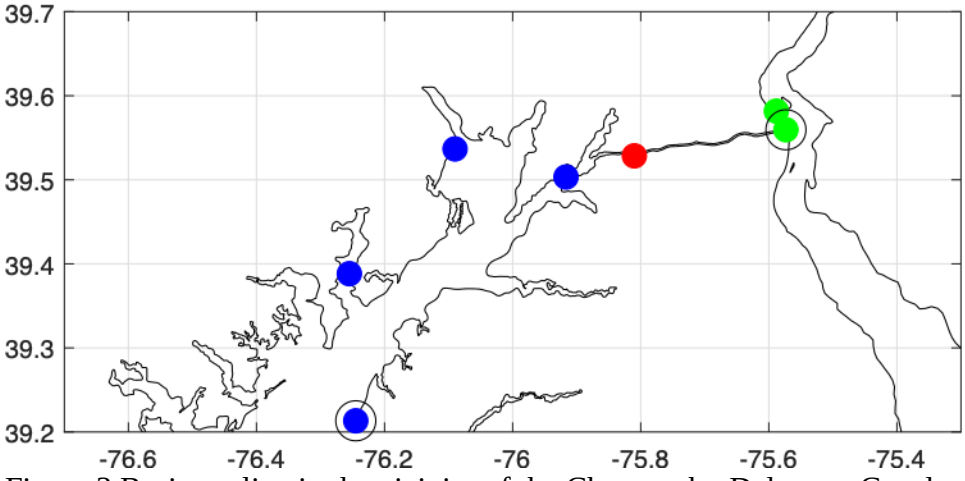

Figure 3 Basin outline in the vicinity of the Chesapeake-Delaware Canal and location of water stations near the west end of the canal (blue; Tolchester Bay gage is circled), east end (green; Reedy Point gage is circled) and at Chesapeake City (red)

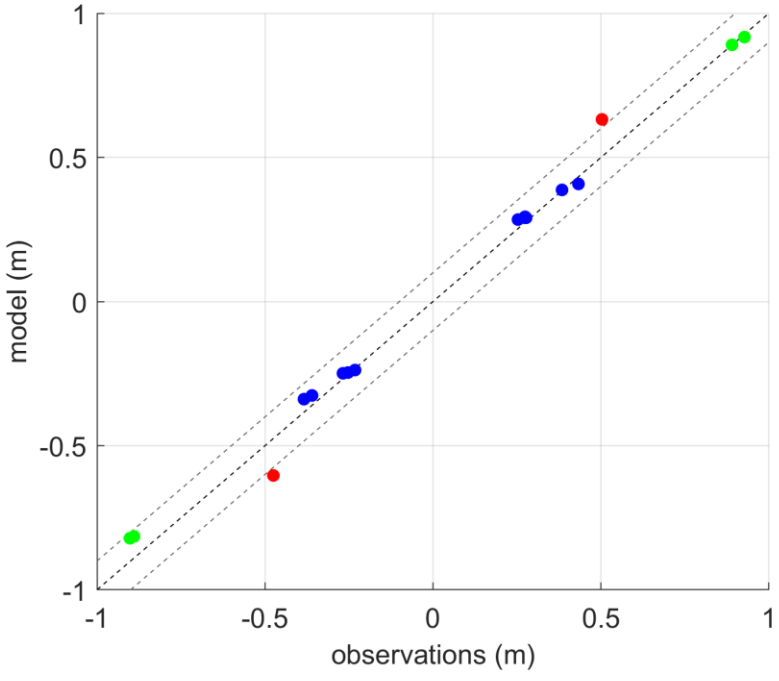

Figure 4 Modeled vs. observed MHHW and MLLW water datums at the stations in the canal vicinity, color-coded according to the gage location as shown in Figure 3. Mismatch at Chesapeake City (datums are overestimated by about 30%) contrasts good match just outside the canal entrances. Dashed gray lines mark 0.1 m up and down deviation from the observations.

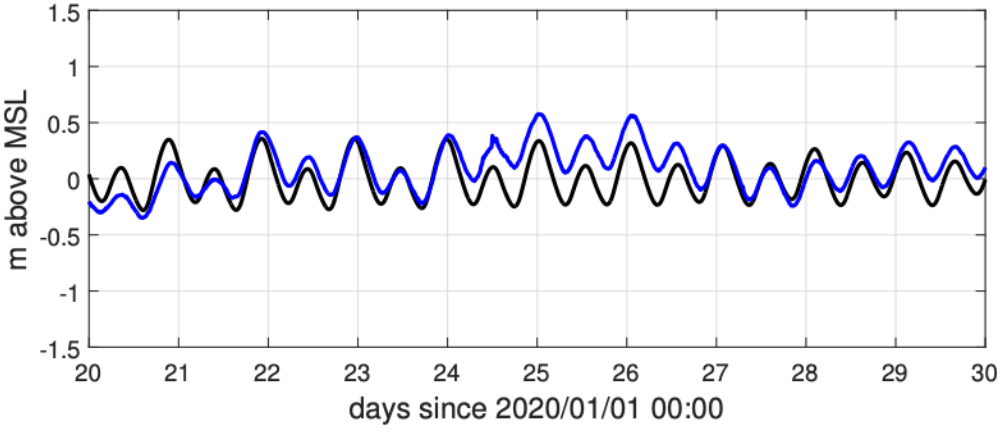

Figure 5 Modeled (black) and observed (blue) tidal time histories at Tolchester Bay water station

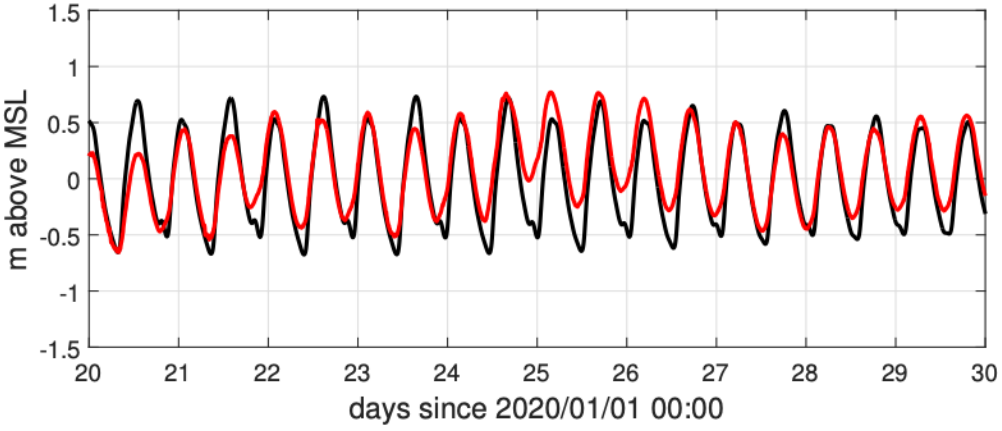

Figure 6. Modeled (black) and observed (red) tidal time histories at Chesapeake City water station

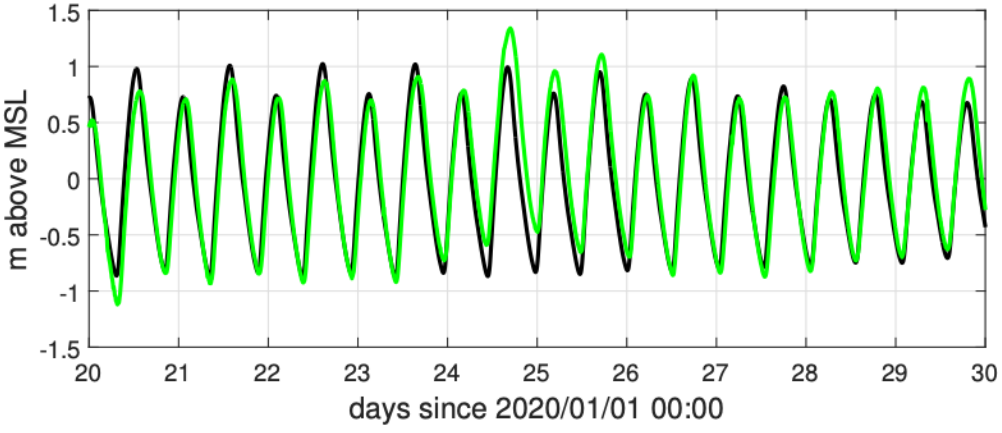

Figure 7. Modeled (black) and observed (green) tidal time histories at Reedy Point water station

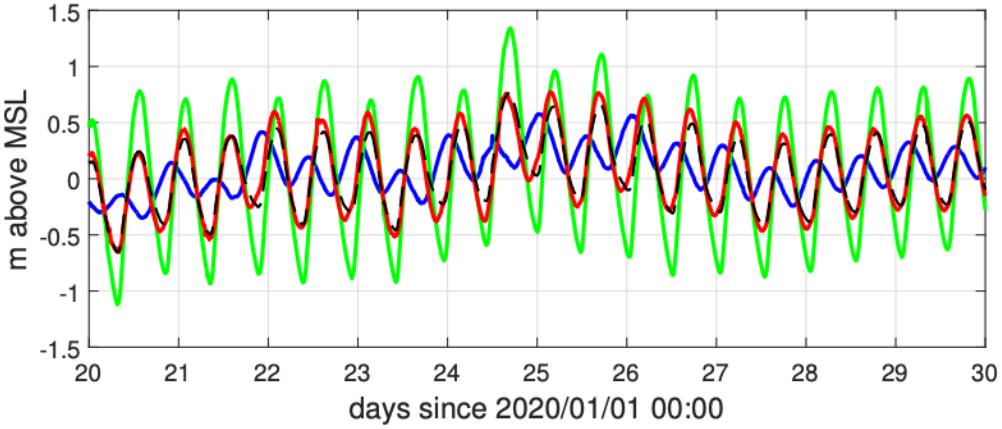

Figure 8 Observed tides at all three locations - Tolchester Bay (TB, blue), Chesapeake City (CC, red), and Reedy Point (RP, green) - and a linear combination 0.48TB + 0.52RP (dashed black) that approximates CC tides

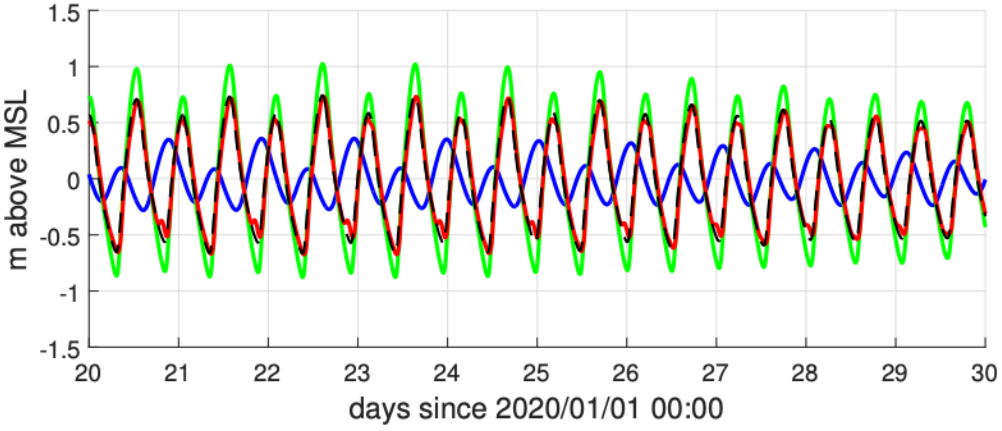

Figure 9. Modeled tides at all three locations - Tolchester Bay (TB, blue), Chesapeake City (CC, red), and Reedy Point (RP, green) - and a linear combination 0.23TB + 0.77RP (dashed black) that approximates CC tides

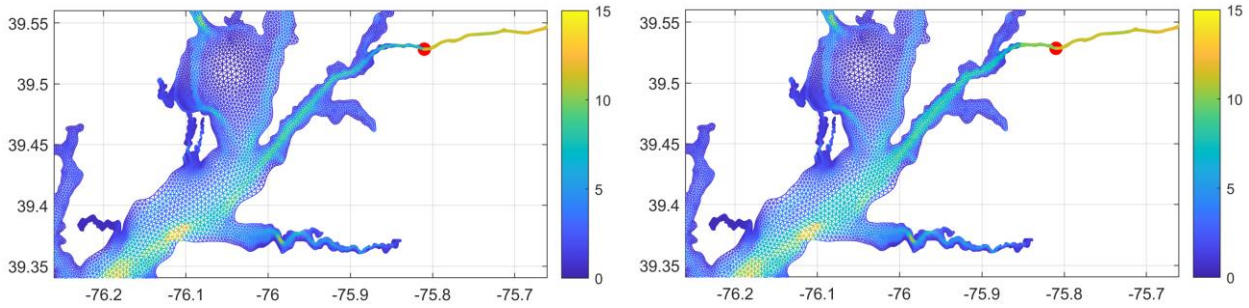

Figure 10. Areal bathymetry in and around the waterway from the Chesapeake Bay to the Chesapeake City (red dot): left the original depth; right that after limiting the minimal depth in the waterway

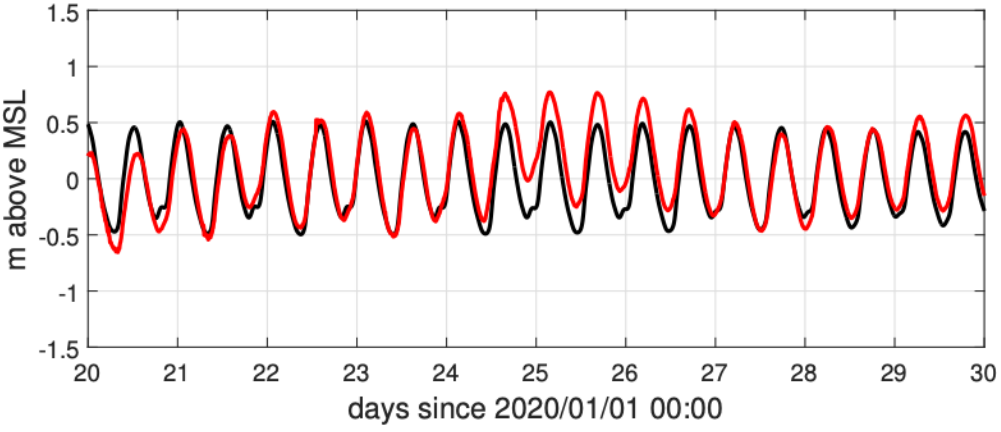

Figure 11. Modeled (black) and observed (red) tidal time histories at Chesapeake City, with the modified bathymetry

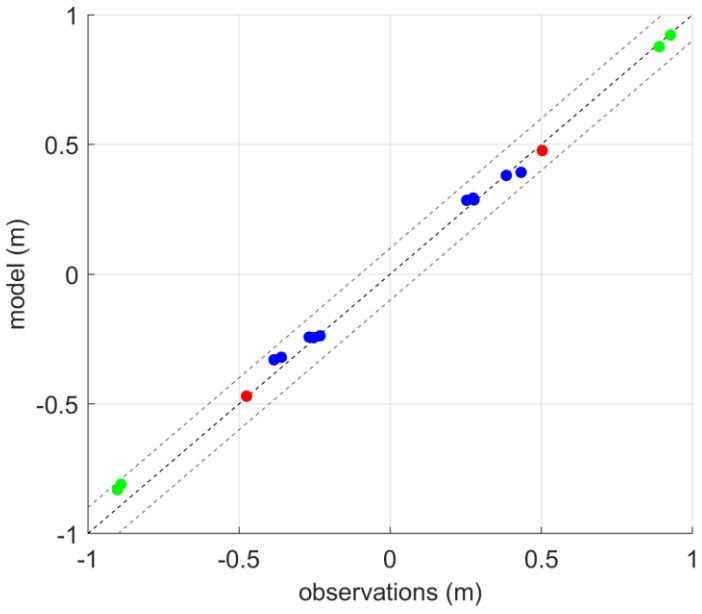

Figure 12. Modeled vs. observed MHHW and MLLW water datums at the stations in the canal vicinity, color-coded according to the gage location as shown in Figure 3, with the modified bathymetry.

3. DATUMS

3.1. Preliminary datums: model-derived

Modeled datums[3] (Mean Higher High Water - MHHW, Mean High Water - MHW, (Local) Mean Sea Level - MSL, Diurnal Tide Level - DTL, Mean Tide Level - MTL, Mean Low Water - MLW, and Mean Lower Low Water - MLLW) relative to the model “zero" were calculated with CSDL’s FORTRAN code ‘lv8j.f’. The input for the code were ADCIRC-modeled water level time histories at 6-minute interval spanning 3 nodal cycles (44.5 days) in duration. Then the datums were re-referenced to the local MSL (by subtracting MSL). Hereafter, all datums refer to those referenced to local MSL. Model-derived tidal fields - MHHW, MHW, MLW, and MLLW

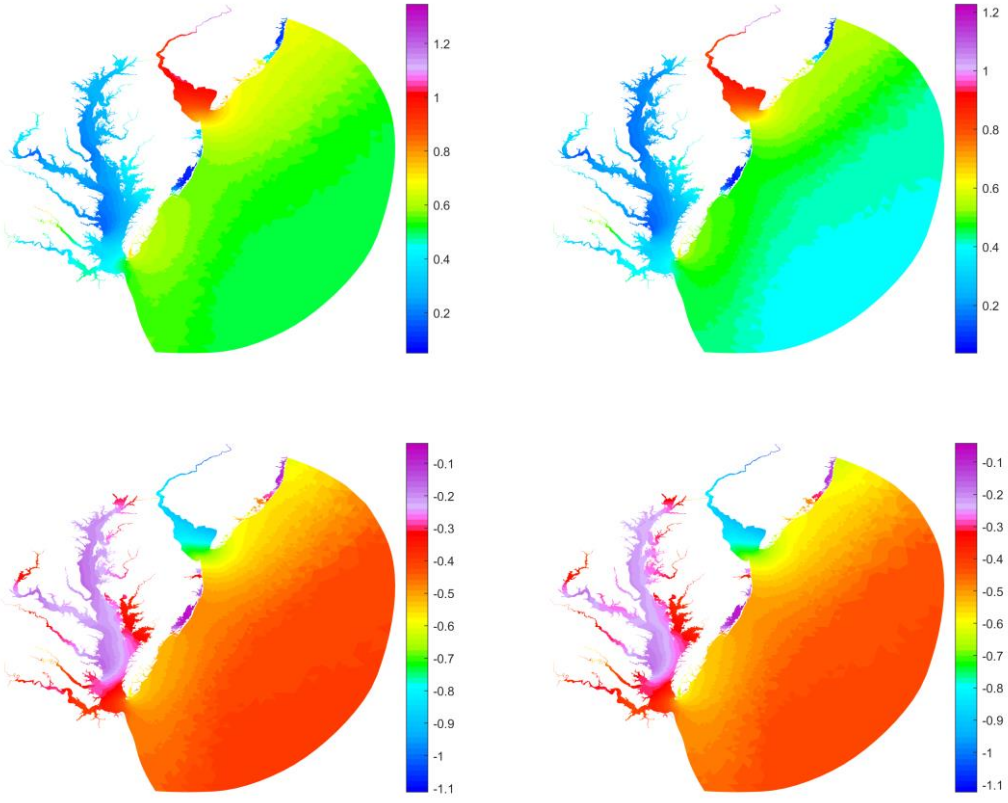

Figure 13. Modeled datum relative to local MSL: MHHW (top left), MHW (top right), MLW (bottom left), MLLW (bottom right); color scale - meters

[3] see https://tidesandcurrents.noaa.gov/datum_options.html for datum definition

- are displayed in Figure 13. Consistent with the previous version of the model, the largest tidal ranges, up to 3 m, occur in Delaware River where tide is amplified upstream by topographical funneling.

3.2. Model validation

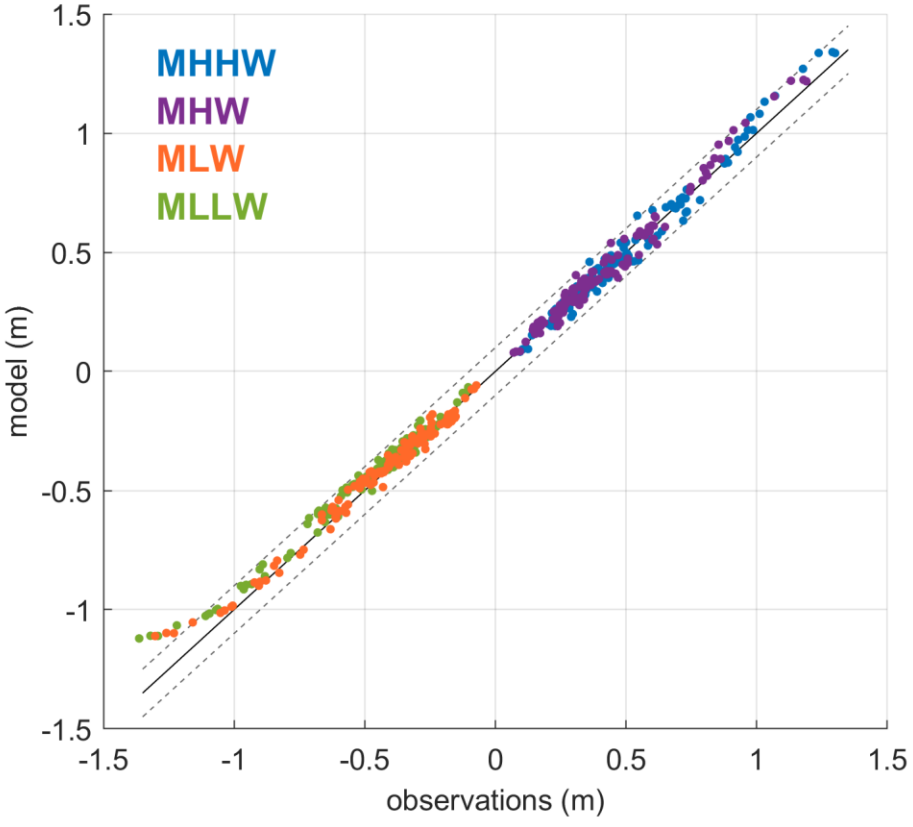

Figure 14. MHHW (blue), MHW(violet), MLW(orange), and MLLW(green) datums, modeled vs. observed. Dashed lines show the error margin of 0.1 m above and below

Both model's parameters tune-up and the model validation are based on comparison between modeled tidal datums and the datums obtained by COOPS from observations at water level stations (tidal gages). Locations of 129 stations used for tuning/validating the model set-up are shown in Fig. 1; and listed in Table 6. The Table also provides the observed datums relative to local MSL. The stations are referenced by their numbers in this report (1-129), and their COOPS 7-digit identification numbers, as shown in Table 6.

Figure 14 displays modeled MHHW, MHW, MLW, and MLLW datum vs. respective observed datums. The datums are color-coded according to the figure legend. Dashed lines show ± 0.1 m error margin. All modeled datums fit within the ± 0.1 m error allowance, but MLW and MLLW at four stations. These four stations are the most upriver stations in the Delaware river, where the tidal ranges are the greatest. Due to model limitations (such as a need to cut a river short at the grid boundary, or lack of provisions for possible river bed elevation above model "zero") and uncertainty of environmental parameters in rivers (such as freshwater discharge, bed friction, or ever-changing bathymetry), the model results in upper river reaches are the least reliable over the model domain. However, assimilation of the observations at the next stage of the datum computations will allow to correct for the model errors.

Visual agreement between modeled and observed water level time histories at selected locations, seen in Figures 5, 7, and 11, also serves as an additional validation of the modeling.
Two more tidal datums - DTL $= (MHHW + MLLW)/2$ and MTL $= (MHW + MLW)/2$ - are entirely determined by the four other datums, and are going to be approximated by the model within the same ± 0.1 m error allowance, except probably at the four aforementioned stations in the Delaware River. Nevertheless, we show DTL and MTL, modeled vs. observed, in Figure 15. As seen in the figure, the model tends to overestimate DTL and MTL, which suggests that the modeled tide in inland basins is more asymmetric than it is in reality.

Table 1 lists statistical parameters - minimum, maximum, arithmetic mean, R.M.S. (square Root of Mean Squared value) - for the modeled and observed datums, as well as for their difference evaluated as observed minus modeled, at the gages. In case of the difference - the model error - the mean absolute error is calculated. Average model-data differences (mean absolute errors) of 3.0 cm, 3.1 cm, 2.8 cm, and 4.2 cm for MHHW, MHW, MLW, and MLLW, respectively, show a possible improvement over the 2008 version of the model where the absolute model-data differences averaged to be 4.1 cm, 3.2 cm, 2.9 cm, and 5.2 cm for the respective datums.

Table 1. The minimum, maximum, arithmetic mean, and R.M.S. for the modeled and observed datums, as well as their difference (observed minus modeled), at the gages. In case of the difference - the model error - the mean absolute error is calculated.

MHHW	min, max	mean	R.M.S.
modeled (m)	0.08, 1.34	0.51	0.58
observed (m)	0.09, 1.30	0.50	0.57
error (cm)	-11.1, 8.7	(abs.err.) 3.0	4.0
MHW	min, max	mean	R.M.S.
modeled (m)	0.08, 1.22	0.44	0.50
observed (m)	0.07, 1.19	0.42	0.48
error (cm)	-10.1, 8.6	(abs.err.) 3.1	3.9
MLW	min, max	mean	R.M.S.
modeled (m)	-1.11, -0.06	-0.43	0.49
observed (m)	-1.30, -0.07	-0.44	0.51
error (cm)	-19.1, 5.8	(abs.err.) 2.8	4.0
MLLW	min, max	mean	R.M.S.
modeled (m)	-1.12, -0.07	-0.45	0.51
observed (m)	-1.36 -0.10	-0.49	0.56
error (cm)	-24.2, 3.5	(abs.err.) 4.2	5.7

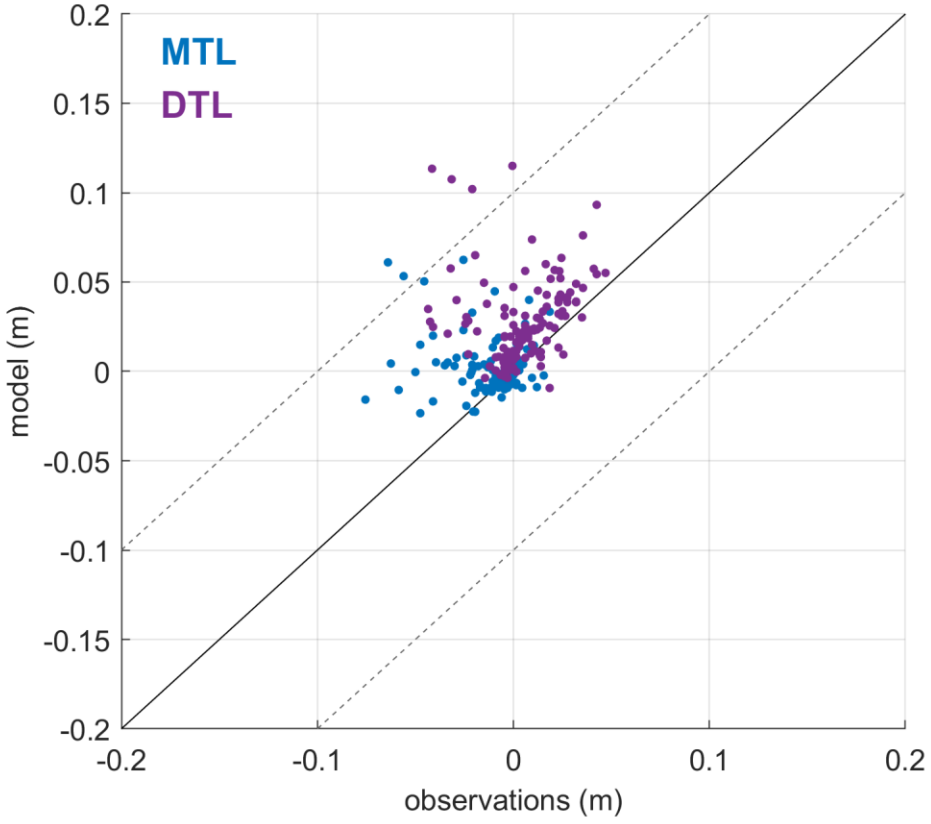

Figure 15. MTL (blue) and DTL (violet) datums, modeled vs. observed. Dashed lines show the error margin of 0.1 m above and below

3.3. Assimilation of observed datums

Once the datums in the domain are calculated using ADCIRC-simulated tidal water levels, these modeled datums are corrected to match the datums observed at the gages using a statistical interpolation method developed by Shi and Myers (2016). After the correction, the final datums agree with the observed ones within 1 cm or an observational error, whichever is greater. The method spatially interpolates the datum errors at gages - that is, differences between observed and modeled datums thought of as a random field - to compute corrections to the modeled datum at all nodes. Thus each final datum $_f$, given by an $N \times 1$ vector of the datum values at N grid nodes, is obtained as:

$$f = f_m + G \cdot (f_o - H \cdot f_m)$$

where f_m is an $N \times 1$ vector of modeled datum values; f_o is an $M \times 1$ vector of observed datum values; H is an $M \times N$ matrix whose rows are made of all zeros except a single 'one' at a node closest to a respective gage, or the so called observation operator which maps the variable from

the model space to the observation space, so $H \cdot f_m$ is an $M \times 1$ subset of modeled datum values at M gages; and G is an $N \times M$ matrix that interpolates/extrapolates datum errors at the gages over the entire domain. Each row of matrix G sums up to one. From the viewpoint of the so called variational data assimilation, matrix G is computed as

$$G = \hat{P}\left(H\hat{P} + R\right)^{-1}$$

where $\hat{P}$ is an $N \times M$ matrix whose columns are maps meant to represent covariance of the datum errors between each gage - one gage per a respective column - and all other nodes; and R is a diagonal $M \times M$ matrix which essentially prescribes permitted deviation of the final datum from the observed datum at each gage location. Variational data assimilation also provides a map of the Spatially Varying Uncertainty (SVU) of each final datum. The details of the method are described in (Shi and Myers, 2016). The method is implemented in MATLAB codes authored by Dr. Lei Shi.

Since the datum error covariance $\hat{P}$ is unknown, its empirical estimates are employed. Currently, CSDL is using Matlab codes in where matrix $\hat{P}$ has a form:

$$\hat{P} = \sigma^2 \cdot P,$$

where σ^2 is the dispersion (the mean square) of the modeled datum errors at M gages, as determined by the difference with the observed datums; each of M columns of P is a map of a correlation coefficient between datum errors at a respective gage and at all other nodes. Thus it is assumed that the uncertainty of the original modeled datum f_m is spatially uniform, unlike that of the final datum $_f$. Next, the correlation coefficient is evaluated as

$$P_{ij} = C_{ij} \cdot S_{ij}, i = 1, \dots, Nj = 1, \dots, M \qquad (1)$$

where C_{ij} is a correlation coefficient between time-histories of tidal extrema envelopes at i-th node and $_j$-th gage; and $S_{ij} = e^{-d_{ij}/L}$, d_{ij} being a distance along the shortest waterway from $_j$-th gage to i-th node, e-fold distance $L = 222$ km. Matrices C and the error standard deviations σ vary among different datums, while the spatial mask S remains the same.

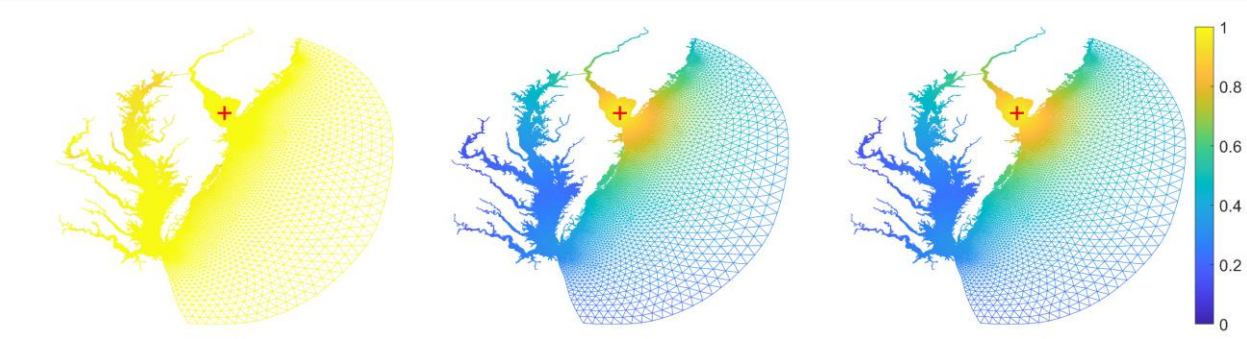

Figure 16. Sample maps contained in a 37-th column of matrix C (left), matrix S (center), and their product matrix P (right). Red cross in the lower Delaware Bay marks location of gage 37.

Figure 16 displays a sample, 37-th column in each of the three matrices: C, S, and P. As seen in the figure, matrix P (right) is almost entirely defined by the spatial mask S (center), with the correlation coefficient C (left) valuing near 1 over most of the grid.[4]
Given that
matrix P is mostly determined by the spatial mask S, and
matrix C introduces multiple unphysical distortions to the final datums as detailed further, such as
generating values outside the range of both the original model datum domain-wide and the observations,
generating spots of chaotic patterns too small-scale to represent tidal variance,
occurrences of positive MLLW, and
occurrences of MLLW above MLW, and MHW above MHHW,
we also attempted datum correction using a simpler matrix P - the same for all four datums:

$$P_{ij} = S_{ij}. \qquad (2)$$

Reducing P to just the spatial mask as in (2) has resolved all the problems above, and resulted in physically sound datums after the data assimilation procedure.
Thus, two sets of final products were computed: one set is obtained with the use of matrix P as in (1), hereafter referred to as long P, which is CSDL-standard; and an alternative datum set obtained with the use of matrix P as in (2), hereafter referred to as short P.

[4] The latter is a very expected result. Imagine that the model is forced with just one tidal constituent. In this case, no matter how tidal time histories evolve within the domain - no matter how attenuated, or amplified, or distorted, or rich with overtides - they remain strictly periodic and thus have all the extrema at the same level, so the extrema envelopes are flat, so their correlation coefficients are all at 100%, so $C_{ij} = 1$ for all i, j.

3.4. Datums after correction with long P

Final tidal fields after the correction - MHHW, MHW, MLW, and MLLW - with long P are displayed in Figure 17.

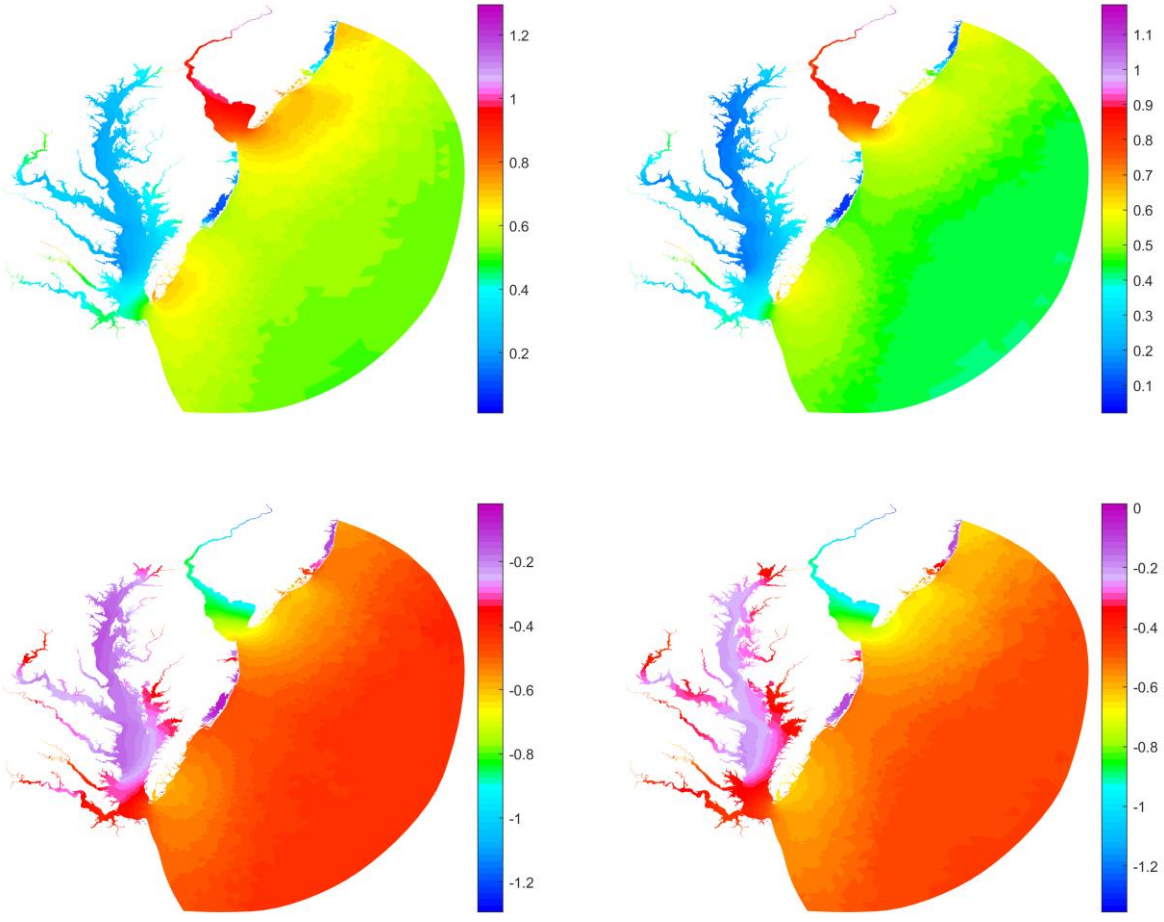

Figure 17. Final tidal datums obtained with long P: MHHW (top left), MHW (top right), MLW (bottom left), MLLW (bottom right); color scale - m

3.5. Datums after correction with short P (alternative)

Final tidal fields after the correction - MHHW, MHW, MLW, and MLLW - with short P are displayed in Figure 18.

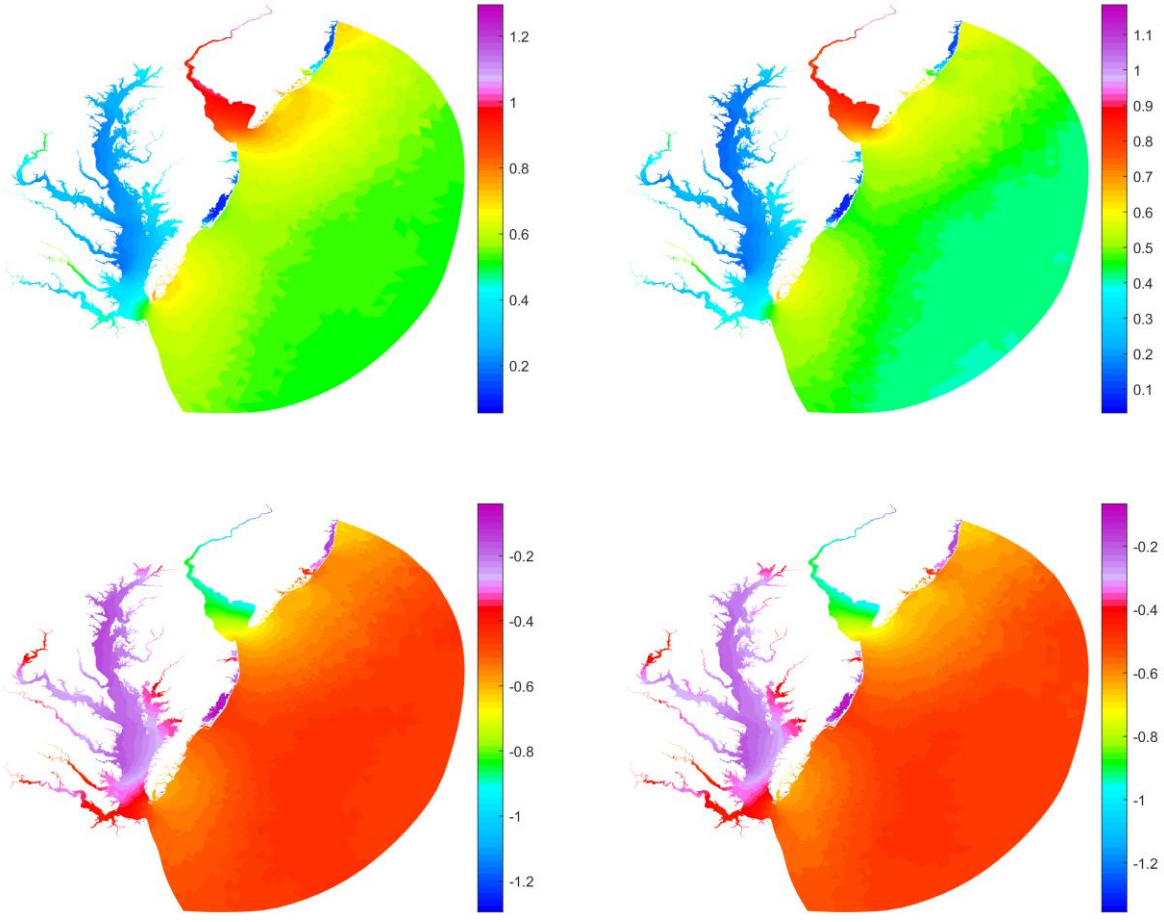

Figure 18. Final tidal datums obtained with short P: MHHW (top left), MHW (top right), MLW (bottom left), MLLW (bottom right); color scale - m

3.6. Comparison between two sets of final datums

The two datum sets in Figures 17 and 18 appear almost identical, yet they are different. Area-wide differences between final tidal datums obtained with short P and long P are displayed in Figure 19. For better visibility, the color scale saturates at ± 5 cm, though the maximal absolute

differences are greater than that and constitute, respectively, 8.3 cm for

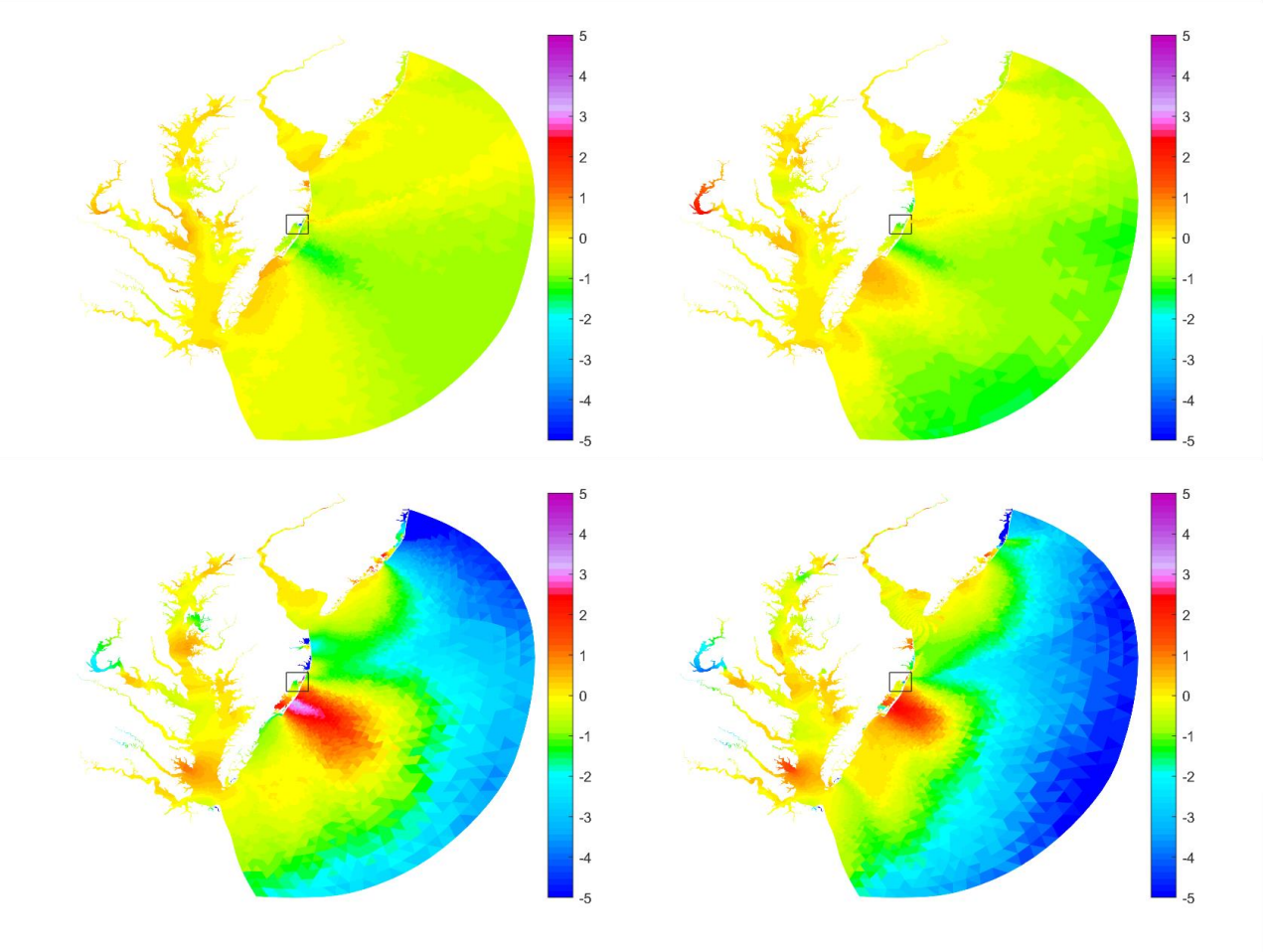

Figure 19. Area-wide differences between final tidal datums obtained with short P and long P (the former minus the latter): MHHW (top left), MHW (top right), MLW (bottom left), MLLW (bottom right); color scale - cm. For better visibility, the color scale saturates below -5 cm and above 5 cm. Black rectangle delimits area around 75.1606W, 38.2300N depicted in the next figure

MHHW, 6.5 cm for MHW, 9.1 cm for MLW, and 13.9 cm for MLLW. These differences are significant compared to the 10 cm accuracy requirement for the final datums, but still

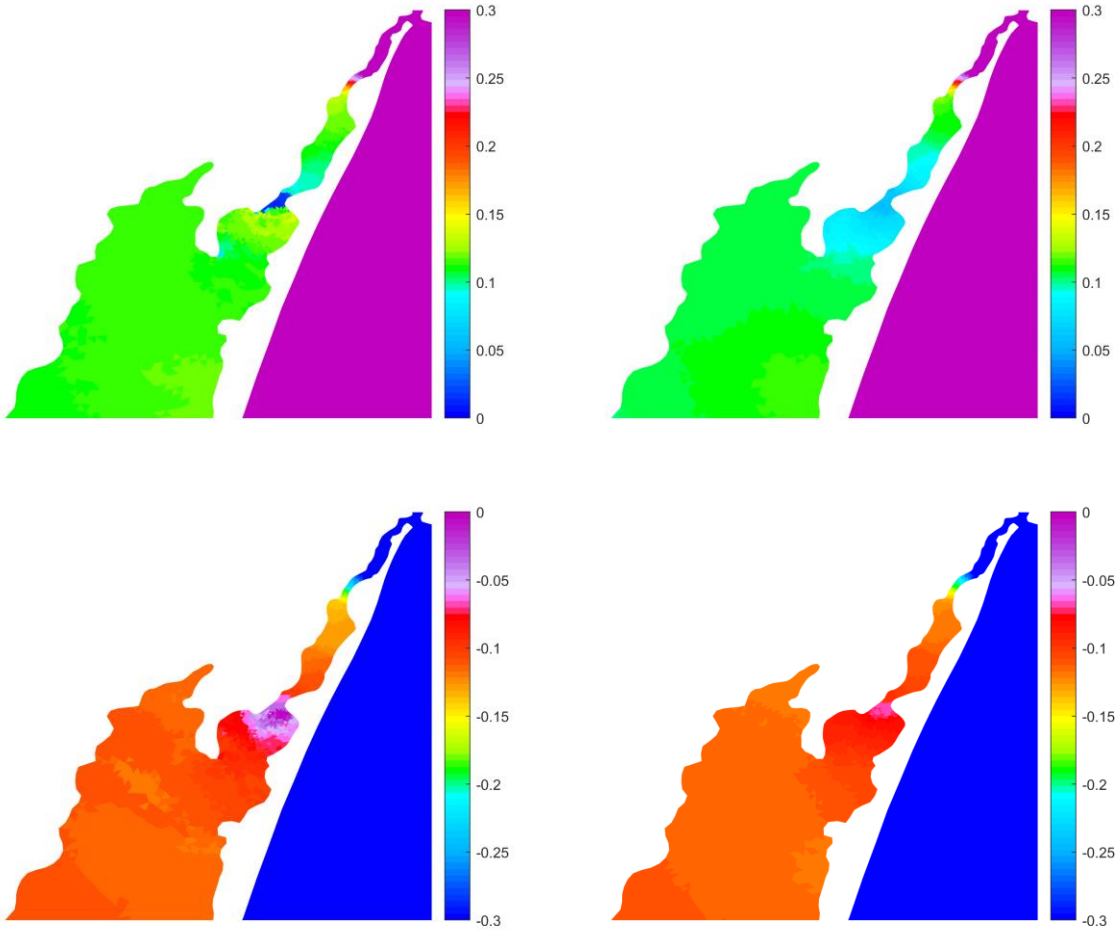

Figure 20. MHHW (top) and MLLW (bottom) yielded with long P (left) and with short P (right) within 20km×20km square around 75.1606W, 38.2300N, on the coast midway Chesapeake Bay and Delaware Bay; color scale - m. The datums with long P (left) display chaotic spotty small-scale pattern, unrealistic for a tidal datum. The datums with short P (right) appear realistic and noise-free (lack of variability offshore is due to color saturation for larger datum values; the color scale is set to better resolve small datum variations in the lagoon)

generates 11 occurrences of positive MLLW (and the use of short P does not generate any). The datums with long P (left) display chaotic spotty small-scale pattern, unrealistic for a tidal datum. The datums with short P (right) appear realistic and noise-free.

Table 2 lists minimal and maximal values over the domain of each of $MHHW$, MHW, $-MLW$, $-MLLW$ as well as $MHHW - MHW$, and $MLW - MLLW$, as directly calculated by ADCIRC the Model, and after correction via long P and via short P, as well as min/max among these datums observed at gages in the region. We see, that long and short Ps yield practically the same results when tidal amplitude is large. In particular, maxima of $MHHW$, MHW, $-MLLW$ and $-MLW$ are almost identical after either P, and modify the modeled datums towards the observations (see the last four columns in the Table). However, when the tidal range is small, the two Ps modify the modeled datum in very different ways (the previous four columns).

Long P dumps the tidal amplitude further, pushing all datums toward zero - contradictory to both observations and the model. Moreover, the datums are bended in unphysical way, with positive MLLW, MLW below MLLW, and MHW above MHHW at some points, as seen in the Table 2. Short P has no such effect. After correction with short P, minima and maxima of all modeled datums, as well as increments between MLLW and MLW, MHW and MHHW, have become closer (or, at least, no further than the model had yielded) to the observed values; and $MLLW \leq MLW \leq 0 \leq MHW \leq MHHW$ holds everywhere.

Table 2. Minimal and maximal values over the domain of each of $MHHW, MHW, -MLW, -MLLW$ as well as $MHHW - MHW$, and $MLW - MLLW$, as directly calculated by ADCIRC the Model, and after correction via long P and via short P, as well as min/max among datums observed at gages in the region.

datum magnitude	gages min	ADCIRC min	long, min	short, min	gages max	ADCIRC max	long, max	short, max
MHHW (m)	0.09	0.050	0.017	0.056	1.30	1.34	1.30	1.30
MHW (m)	0.07	0.037	0.025	0.033	1.19	1.23	1.19	1.19
-MLW (m)	0.07	0.040	0.02	0.04	1.30	1.11	1.30	1.30
-MLLW (m)	0.10	0.043	**-0.025**	0.067	1.36	1.12	1.36	1.36
MHHW-MHW (cm)	2.4	0	**-1.9**	0.01	13.4	12.6	13.7	13.6
MLW-MLLW (cm)	1.7	0.3	**-8.1**	1.7	7.7	7.1	12.5	7.7

4. MARINE GRIDS

4.1. Bounding polygons and marine grids

The model domain spreads from the state of New Jersey (NJ) on the North to North Carolina (NC) on the South, and passes through the states of Delaware (DE), Maryland (MD), and Virginia (VA). This area was covered by seven bounding polygons shown in Figure 21. The above polygons define seven VDatum sub-regions in the model domain, to be populated with the datum interpolated onto rectangular GTX grids. The regions bounded by the polygons are named with 10-symbol words, as listed in Table 3. The polygons have been developed in such a way that

- the polygons cover all inland basins connected to the ocean, up to the farthest inland water level stations and up to the boundaries of the neighboring VDatum regions;
- the polygons do not overlap with each other nor the polygons from the neighboring regions;
- the polygons include dry land adjacent to the included waters up to at least 500 m from the shoreline;
- the polygons exclude narrow channels upriver of the farthest inland gage;
- offshore polygon boundary is the same as that for the 2008 model;
- open ocean and coastal lagoons separated by narrow land barriers are placed in different polygons.

For comparison, Figure 22 shows bounding polygons for the original version of the model of 2008. The original bounding polygons and corresponding GTX grid parameters extracted from /disks/NASWORK/vdatum/V/C/ and listed in Table 4. As seen in the figures, the first four regions for the current model are approximately the same as for the original model, so their names are kept the same, but with the next version number. The fifth region of the original model, covering the entire Chesapeake bay with its tributaries, has been divided into three smaller regions in the current model, with an objective to increase resolution in the corresponding GTX grids and improve representation of complex topographic features. The updated, more “loose" bounding polygons allow for extending VDatum coverage farther onto the land and into a greater number of small water bodies next to the coast and the riverbanks. At the same time, the coverage was reduced in the Pamunkey river, Mattaponi river (the tributaries of the York river, VA), Pocomoke river, MD, Nanticoke river, MD, and Choptank river, MD. Due to model limitations (such as a need to cut a river short at the grid boundary, or lack of provisions for possible river bed elevation above model "zero") and uncertainty of environmental parameters in rivers (such as freshwater discharge, bed friction, or ever-changing bathymetry), the model results in upper river reaches are the least reliable over the model domain. Therefore, VDatum coverage in rivers is terminated at or shortly after the most upriver gage used for the model validation.

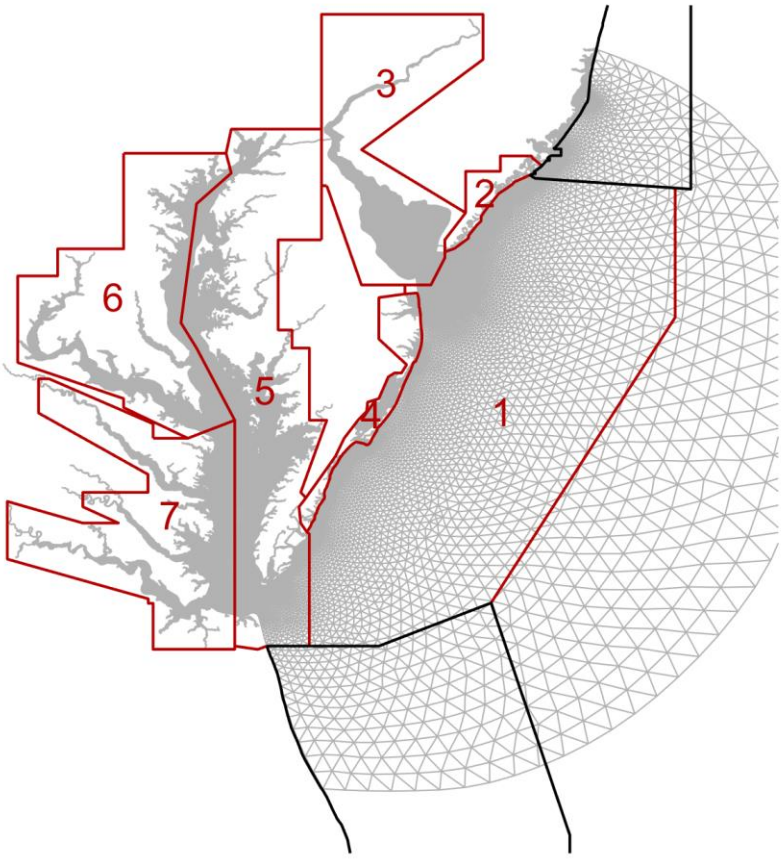

Figure 21. Bounding polygons delimiting seven regions in the model domain (red), and two adjacent bounding polygons from neighboring domains (black) that share wet interfaces. Bounding polygon 3 encloses the Delaware Bay and the Delaware river estuary. Bounding polygons 5-7 cover the Chesapeake Bay and its many tributaries.

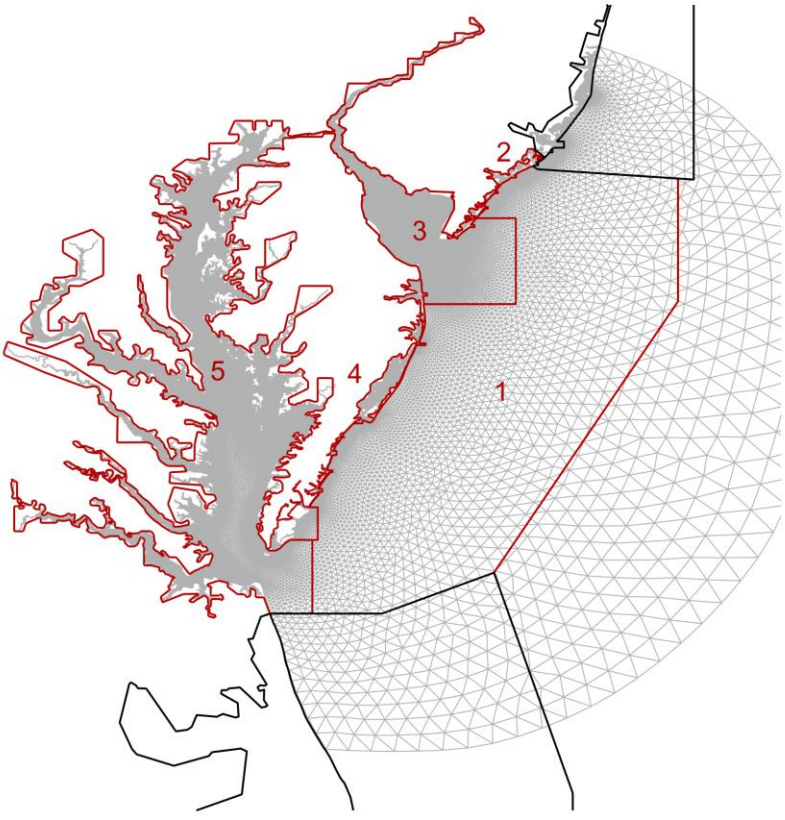

Figure 22. Bounding polygons delimiting five regions in the 2008 model domain (red), and adjacent bounding polygons from neighboring domains (black)

The model domain touches four VDatum regions named, respectively, *NYNJbays01* and *NYharbor02* on the North, and *NC_inner01* and *NC_coast01* on the South. However, only two bounding polygons from the neighboring models have wet interfaces with the current model polygons: *NYharbor02* shares wet boundary with regions 1 and 2, and *NC_coast01* shares wet boundary with regions 1 and 5.

Table 3. GTX grid parameters for seven sub-regions in the model domain: sub-region name, marine grid resolution along longitude (x) in decimal degrees (first value) and meters (second value), the same - along latitude (y), grid size $nx \times ny$, total number of nodes in the grid, and the number of layers added by vgridder.

	sub-region	x-spacing (deg lon, m)	y-spacing (deg lat, m)	nx, ny	nodes, total	added layers
1	DEmidatl03	0.0025, 219	0.0020, 222	853 x 1311	1118283	3
2	DEnjshor03	0.0007, 60	0.0005, 56	806 x 1139	918034	9
3	DEdelbay03	0.0020, 172	0.0020, 222	469 x 754	353626	3
4	DEmdshor02	0.0012, 105	0.0010, 111	671 x 1387	930677	5
5	MDchesbayE	0.0012, 105	0.0010, 111	705 x 2891	2038155	5
6	MDchesbaNW	0.0010, 87	0.0008, 89	1253 x 1981	2482193	6
7	VAchesbaSW	0.0016, 141	0.0012, 133	823 x 1255	1032865	4

Table 4. GTX grid parameters for five sub-regions of the original model of 2008: region name, marine grid resolution along longitude (x) in decimal degrees (first value) and meters (second value), the same - along latitude (y), grid size $nx \times ny$, and total number of nodes in the grid.

	region	x-spacing (deg lon, m)	y-spacing (deg lat, m)	nx, ny	nodes, total
1	DEmidatl02	0.0040, 352	0.0040, 445	746 x 883	658718
2	DEnjshor02	0.0020, 172	0.0020, 222	286 x 272	77792
3	DEdelbay02	0.0020, 172	0.0020, 222	631 x 876	552756
4	DEmdshor01	0.0020, 175	0.0020, 222	466 x 801	373266
5	DEchesby01	0.0020, 176	0.0020, 222	951 x 1851	1760301

4.2. Match with tidal datums in adjacent areas

Mismatch between datums computed by different regional models in their overlapping areas can be caused by a number of reasons, including (but not limited to) the following:
wave formation simulated by different regional models is affected by different topographic features;
different models might use different selection of tidal forcing and/or different approach for computing datums with a several-week worth of synthetic data;
resulting datums are subjected to adjustments for matching observations at tidal stations in the region, so the datums might be modified differently on different sides of the boundary.
Below, the datums computed by the current model are examined for continuity across the boundary with the neighboring regions populated from different models. Figures 23 and 24 show absolute value of the datum difference, as computed by *test_cont15*[5], along the boundary with *NYharbor02* on the North, and *NC_coast01* on the South, for MHHW, MHW, MLW, and MLLW datums, with the use of either matrix P at the data assimilation step, respectively. The datum differences were calculated at 0.002 arc-deg interval along the wet interface between the regions.

Table 5. R.m.s. of differences of MHHW, MHW, MLW, and MLLW across boundaries of VDatum regions neighboring on the North and on the South, after the data assimilation step with the use of either matrix P; for the present model, and for the 2008 version of the model as shown in the model report, before the correction for the boundary discontinuities.

		MHHW	MHW	MLW	MLLW	MHHW	MHW	MLW	MLLW
			2022	(cm)			2008	(cm)	
North	long P	2.1	2.4	0.7	0.9	1.1	2.5	1.9	1.4
North	short P	2.2	2.5	1.9	2.1	-	-	-	-
South	long P	3.1	2.2	0.8	2.0	3.1	2.1	0.6	3.1
South	short P	3.3	2.7	0.5	1.2	-	-	-	-

[5] The code to test datum continuity across the common boundary of neighboring bounding polygons

As seen in Figures 23, datums computed in neighboring regions are very close (under 1.5 cm different, for both HW and LW, with either *P*) across the northern boundary within about 50 km from the coast, where the datums are well constrained by the observations. Farther offshore, however, discontinuity of both HW datums grows sharply and exceeds 5 cm at the northeast corner of the bounding polygon. The MHHW datum discontinuity across the northern boundary can also be seen in Figure 25, right pane, which shows MHHW datum of the present model and in *NYharbor02* region of the neighboring model, near the two models' interface.
Differently from the North, the HW datums difference across the southern model boundary is maximal - about 3 cm - at the shore. Both LW datums are fairly close to their values in the neighboring regions (Figure 24).

The previous version of this model reports comparable r.m.s. errors across the boundaries with the adjacent regions, and the same difference in how the discontinuity in HW datums is distributed on the North and the South. In the 2008, the final datum was modified to match the existing boundary values in the same manner as it was forced to match the observations: "Tidal datum corrections are applied to the modeled tidal datums to eliminate model-data differences at observational stations as well as to diminish datum discrepancies across boundaries of different VDatum domains... both the observational stations and the domain boundary discrepancies are treated equally as control stations."

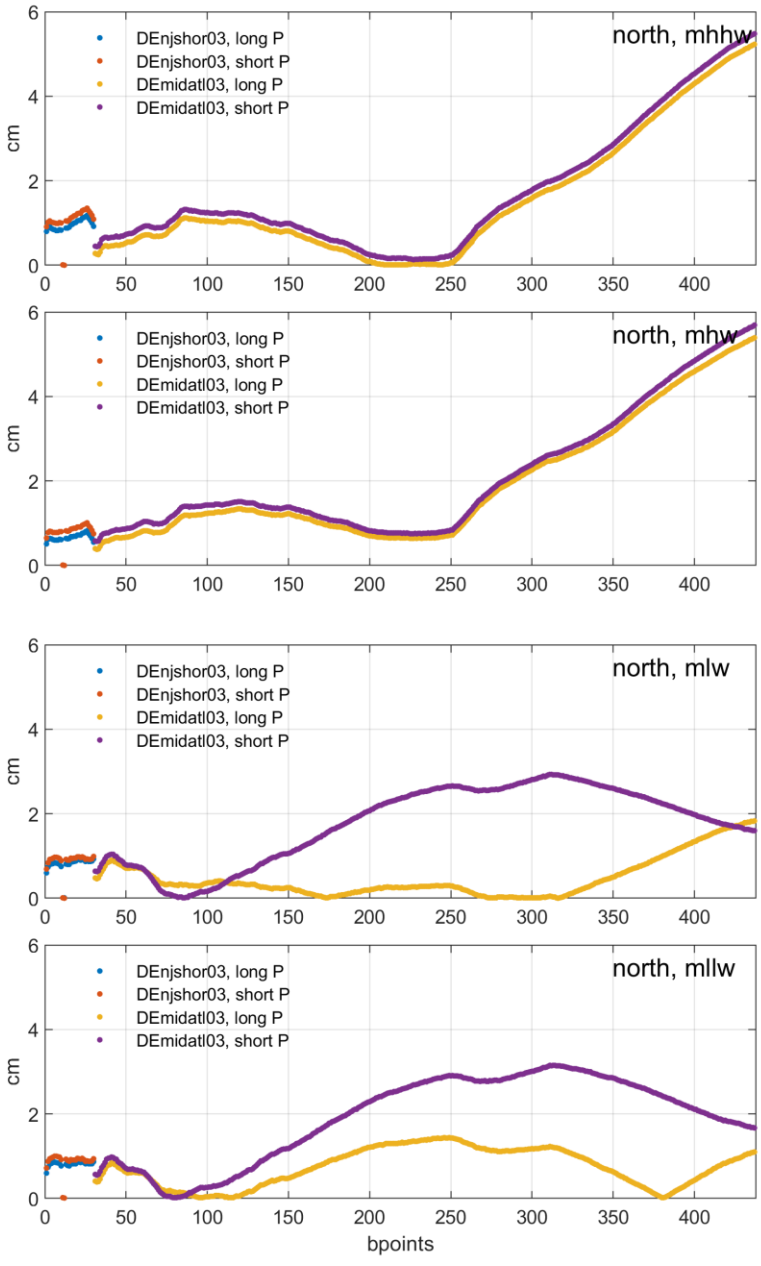

Figure 23. Absolute difference in the four datums between the current model and the adjacent region NYharbor02, at 0.002 deg interval along the model northern boundary; color-coded according to the sub-regions of the current mod el

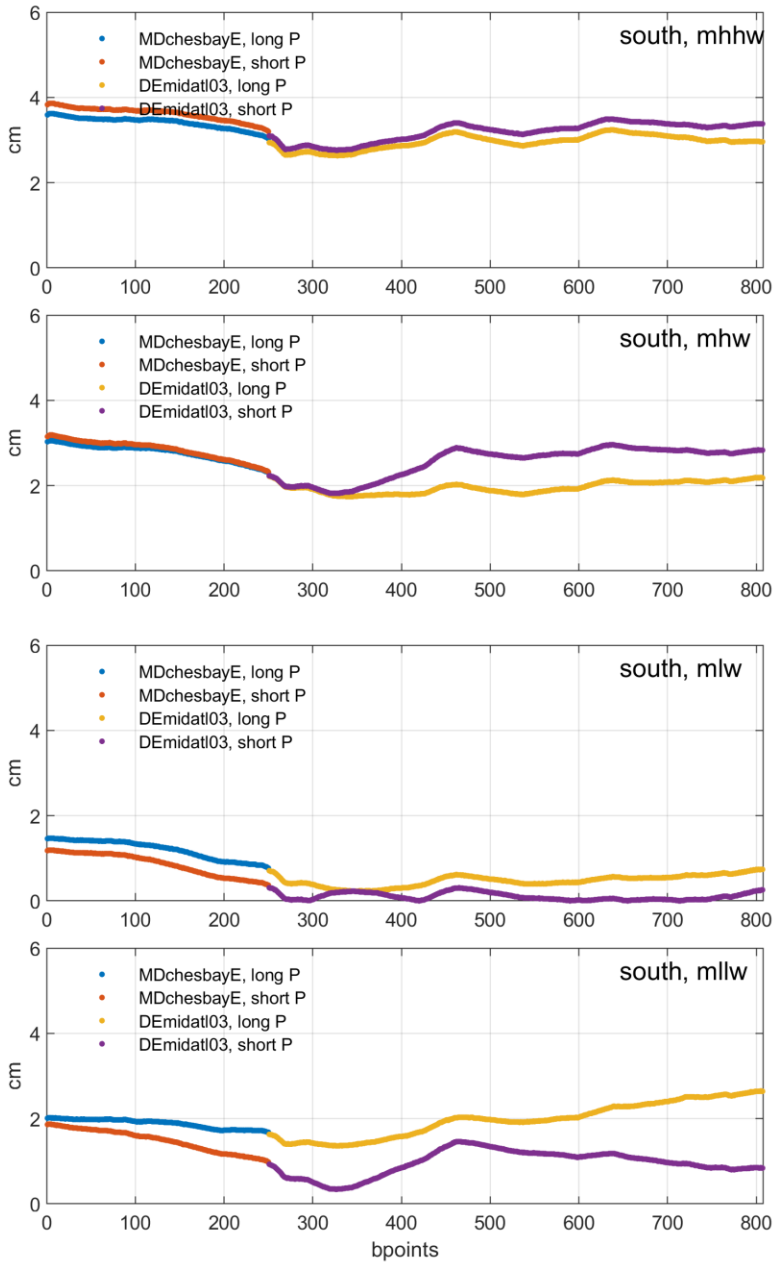

.

Figure 24. Absolute difference in the four datums between the current model and the adjacent region NC_coast01, at 0.002 deg interval along the model southern boundary; color-coded according to the sub-regions of the current model

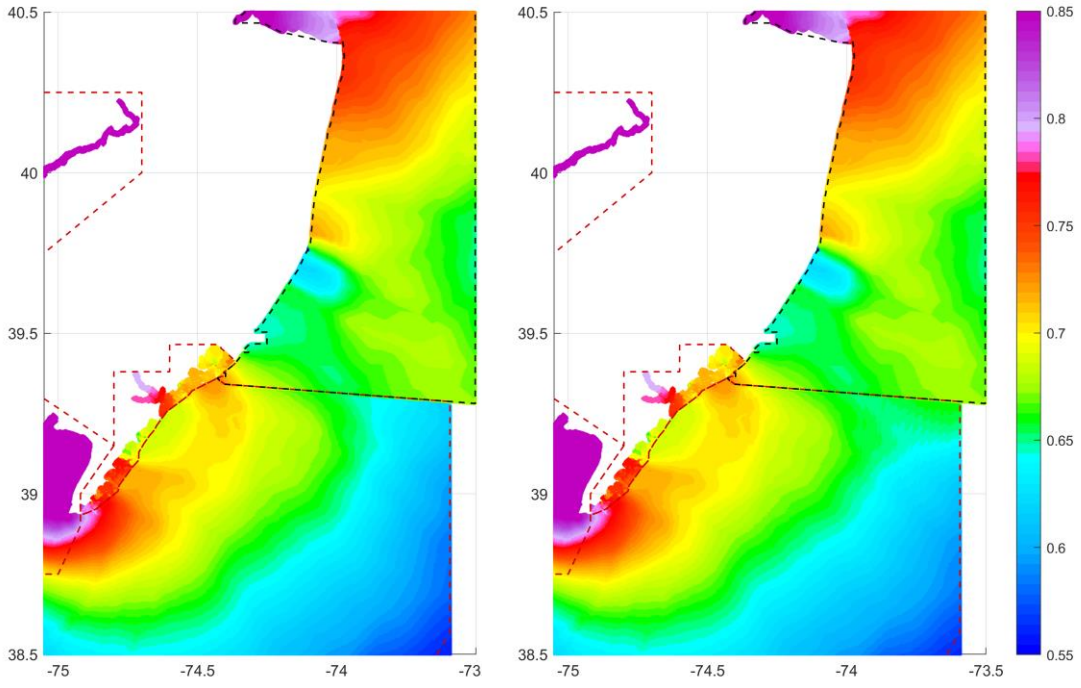

Figure 25. MHHW datums in the vicinity of the Northern boundary between the models, shown in full or partial regions 1-3 of the current model (delimited by dashed maroon lines) and in NYharbor02 of the neighboring model (delimited by dashed black line). The datum values are given by a color-scale which saturates below 0.55 m and above 0.85 m, to contrast the datum difference along the models' interface. We indeed observe datum discontinuity across the boundary farther offshore (left), which is removed after locally-applied correction (right)

4.3. Investigation of High Water datums discontinuity on the model's North

Figure 26 shows the final MHHW datum from the 2008 in a sub-region encompassing the interfaces with the neighboring VDatum regions. It appears, that smoothing the datum difference across the northern boundary had resulted in displacing the discontinuity inside the grid, with the size of the discontinuity being the same 5 cm in the same area, as in the current model. Apparently, there has to be a physical reason inherent in the model set up that is responsible for this discontinuity persistently arising in the same location.

A look at the MHHW datum over a larger area in the neighboring model (see Fig. 27) suggests a possible explanation for this discontinuity. Above the current model domain, the continent and

the Long Island form a roughly right angle bordering the NY/NJ Bight. Tides in the Bight are amplified by this topographic feature, with its effect felt over 100 km from the vertex. In particular, if this amplification spreads toward the northeast of the current model domain, it can cause higher datums north of the current model boundary. At the same time, the effects of this topographic feature can't be accounted for in any version of the present model which domain does not include the Long Island.

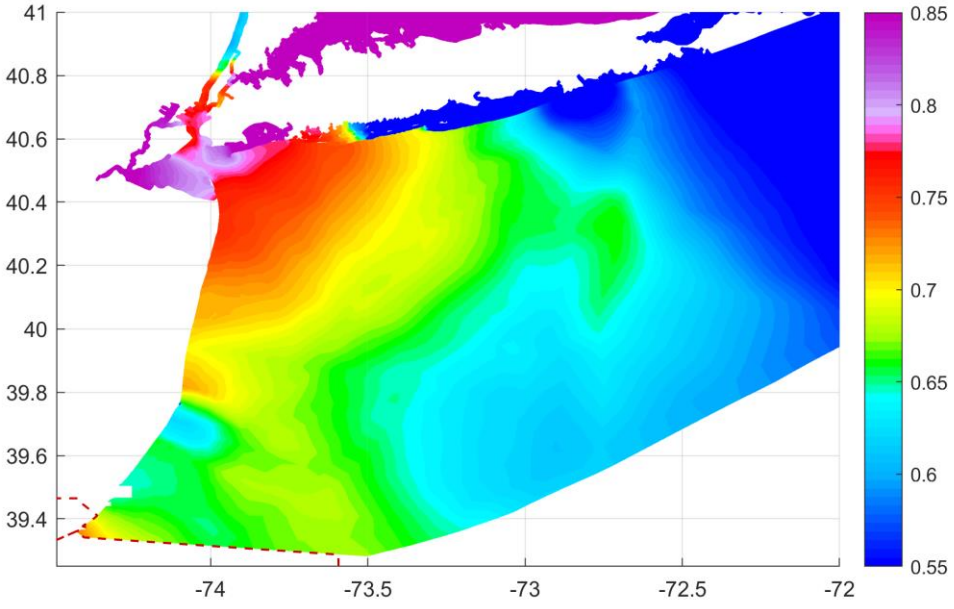

Figure 26. MHHW datums in the neighboring model in regions NYgrsoby02, NYlisnyb02, NYharbor02. Dashed maroon lines delimit adjacent regions 1 and 2 of the current model

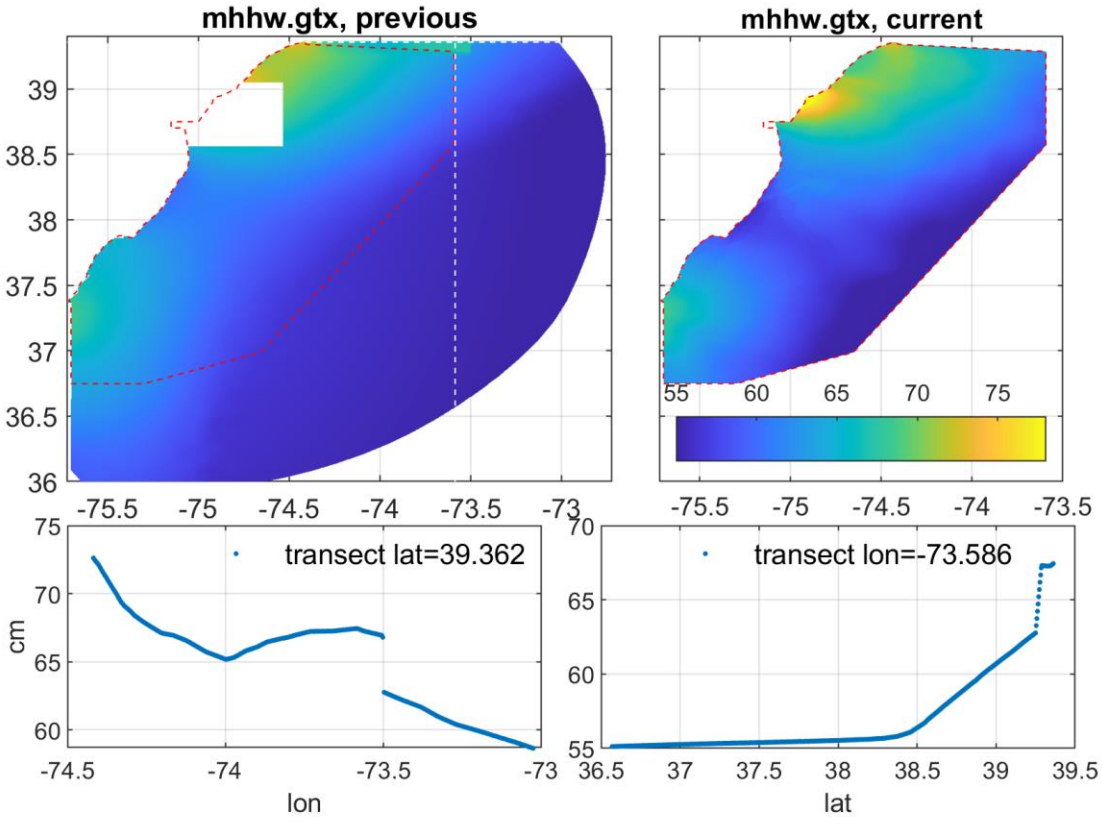

Figure 27. *top left*: The final MHHW datum from the 2008 model, as found in the VDatum repository (disks/NASWORK/vdatum/M ... /DEdelches01), with the bounding polygon for sub-region 1 of the present model (dashed red) and transects shown in the bottom plots (dashed white lines) ; *top right:* present MHHW datum in the sub-region 1; *bottom:* 2008-datum transects along the top edge of the grid, west to east *(left)*, and across it, south to north *(right)*

Therefore, the only way to exclude the discontinuity is to force the match at the boundaries by altering the datum in some way. However, we anticipate spatial scales of boundary discrepancies be quite different (smaller) than the correlation radius of a datum field, therefore we can't treat boundary discrepancies "equally with the control stations" for the statistical correction (SVU) method. Instead, a localized correction to each HW datum was applied, by subtracting the boundary error exponentially diminishing with the distance from the boundary, with e-fold length of 30 km. The resulting MHHW datum, altered near the northern boundary in *DEmidatl03* subregion, is shown in Figure 25, left. Similar correction was applied to all four datums derived with short P, and to MHHW and MHW datums derived with long P. After the correction, discontinuity in any datum across the northern boundary does not exceed 2 cm.

4.4. Investigation of High Water datums discontinuity on the model's South

While the discontinuity at the North makes physical sense, the discontinuity at the South looks suspicious because it is largest at the coast. Near the coast, datums are well constrained by the gages. Near the coast at the southern boundary at particular, the datums are constrained by stations 8639208 at roughly 10 km North of the boundary and 8639428 at roughly 10 km South of the boundary, with straight open coast in between. MHHW datum observed at station 8639208 is 57.3 cm; MHHW observed at station 8639428 is 59.7 cm; therefore, we expect MHHW at the landward end of the boundary be in-between these values, around 58.5 cm. MHHW datum at this end of the boundary computed here is 59 cm which appears reasonable; whereas MHHW datum at the adjacent point in the neighboring model is 62 cm which is outside the expected range. That neighbor's MHHW datum near the boundary deviates from the observations is seen in Figure 28, right pane, where circles representing observed datums at the gages are colored differently than their surroundings representing neighbor's MHHW (but away from the boundary, the agreement with the observations is restored).

Thus the observational data suggest that HW datums by the present model are more accurate, and therefore no datum correction has been done at the south boundary.

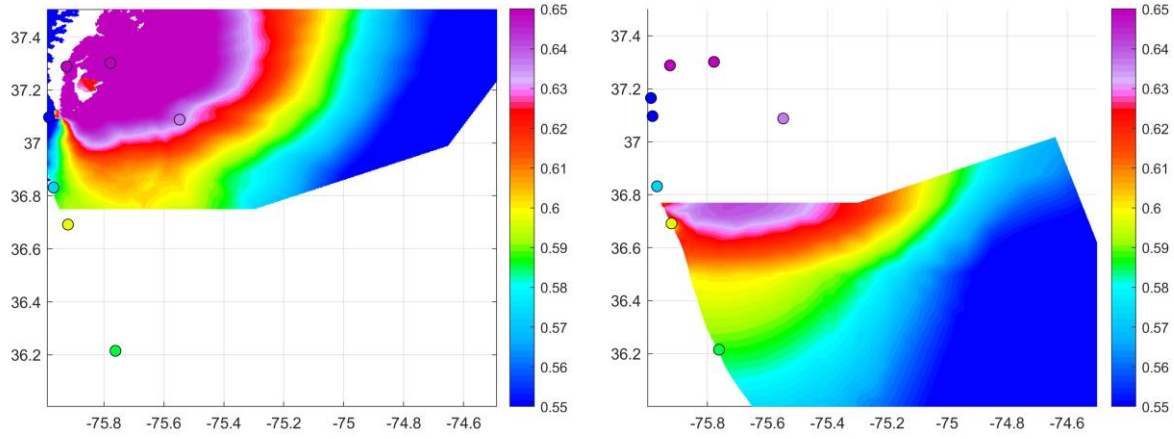

Figure 28. Zoom onto MHHW near boundary between the current model (left) and the neighboring NC_coast01 (right); circles denote gages color-coded according to the observed MHHW; color scale - meters (color scale is selected to better resolve the datum variation along the boundary, and saturates in other regions)

4.5. Populated marine grids

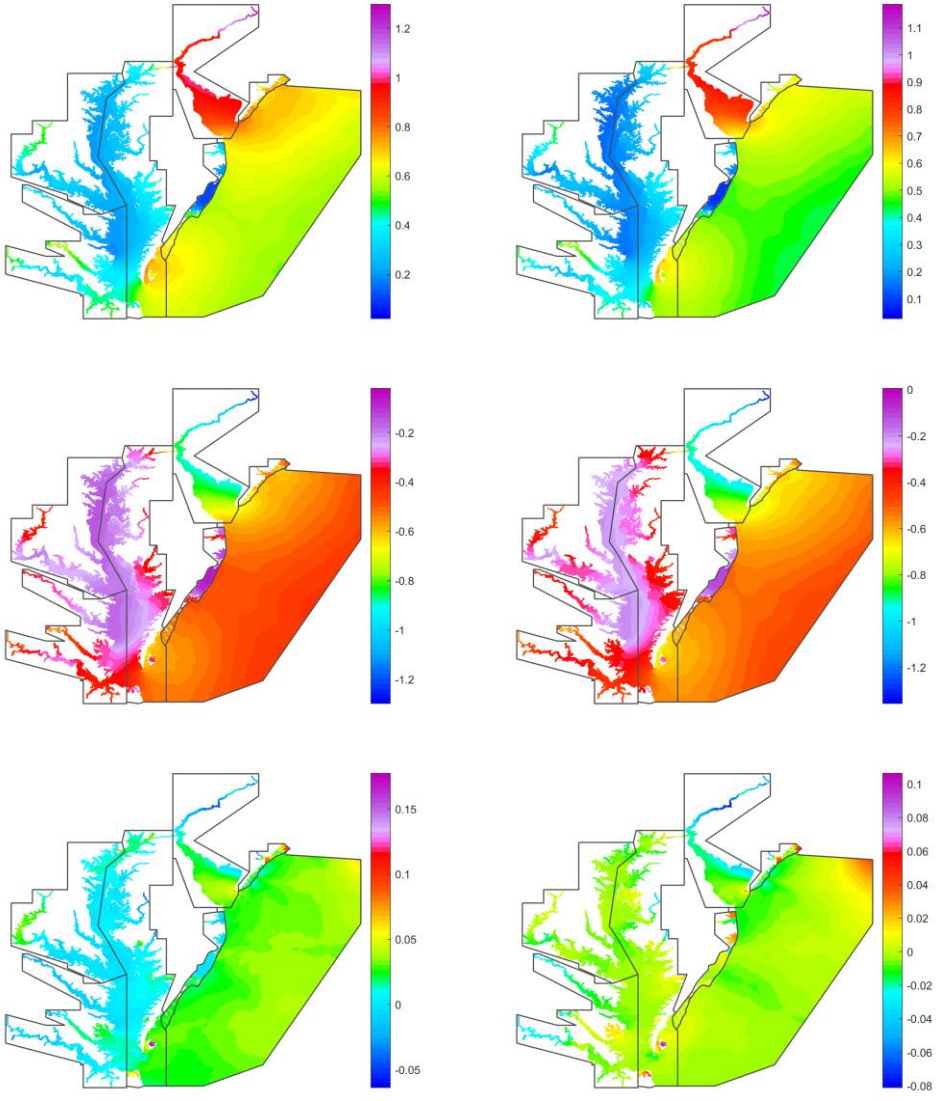

Figure 29. Modeled datums relative to local MSL interpolated onto seven marine grids: MHHW (top left), MHW (top right), MLW (middle left), MLLW (middle right), DTL (bottom left), MTL (bottom right); color scale - meters; long P

After all applicable adjustments, marine grids populated with six tidal datums are shown in Figure 29 (long *P*) and Figure 30 (short *P*). Spatially-varying uncertainty (SVU) estimate yield by the statistical interpolation method is shown in Figure 31. Note, that SVU represents the

lower estimate for the standard deviation of the datum error, under a number of assumptions about the error statistics. As SVU for any datum is under 4.5 cm, the lower estimate for the 95% confidence interval of the computed datums is 9 cm. This is under 10 cm allowance.

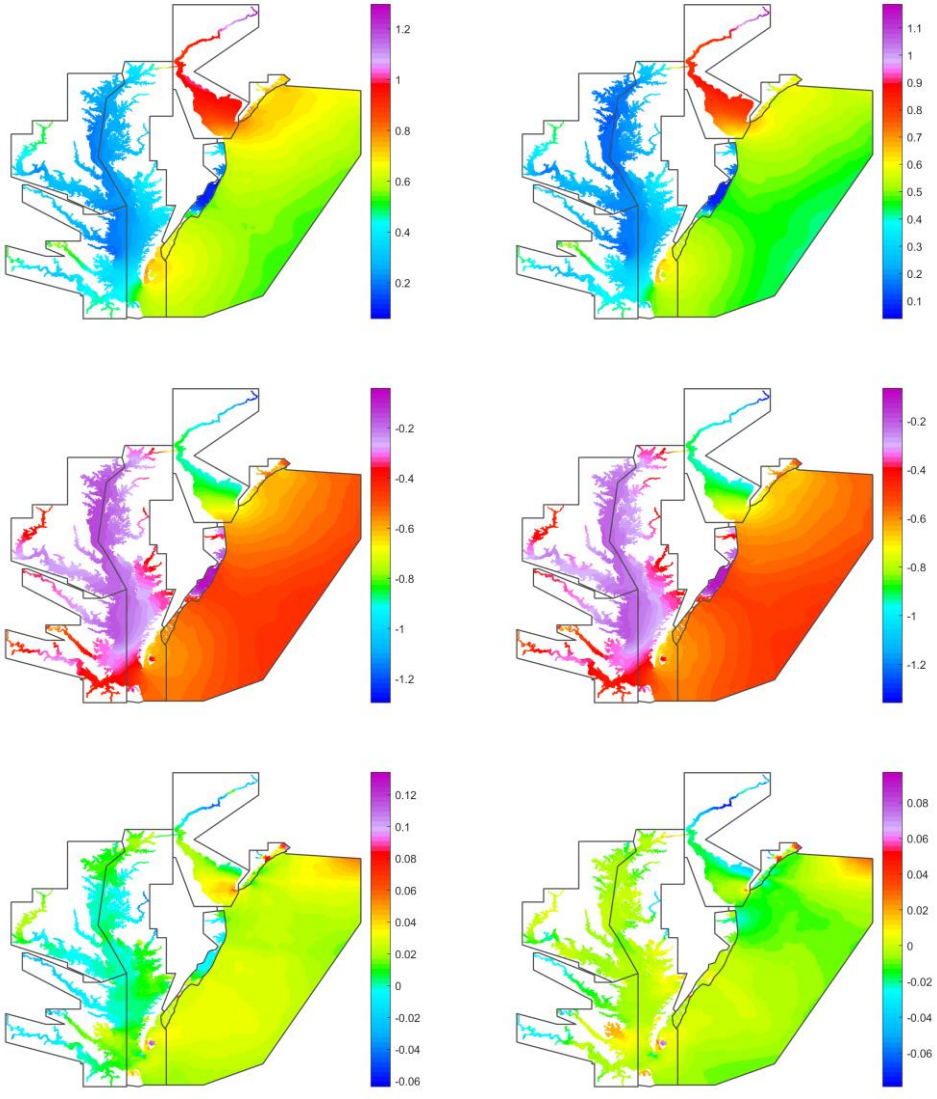

Figure 30. Modeled datums relative to local MSL interpolated onto seven marine grids: MHHW (top left), MHW (top right), MLW (middle left), MLLW (middle right), DTL (bottom left), MTL (bottom right); color scale - m; short P

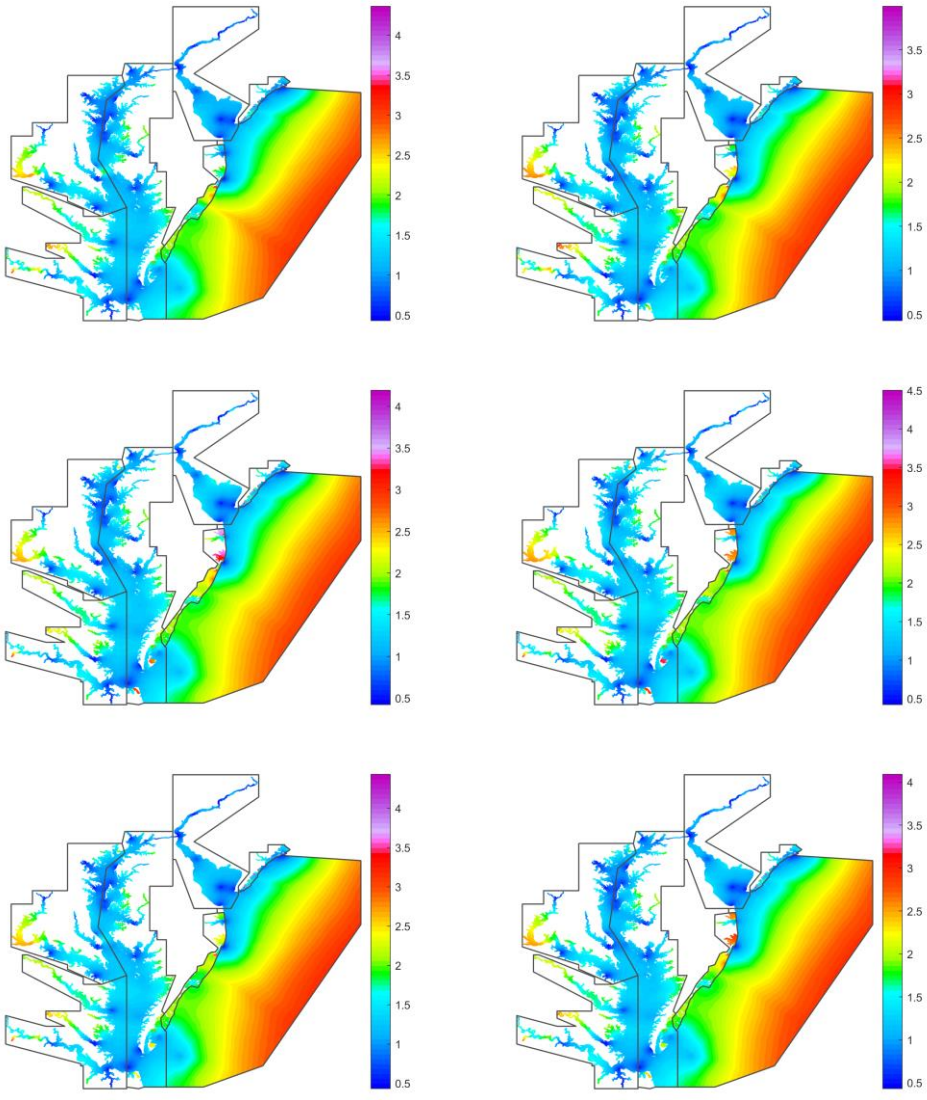

Figure 31. Spatially varying uncertainty (SVU) interpolated onto seven marine grids, for each datum type: MHHW SVU (top left), MHW SVU (top right), MLW SVU (middle left), MLLW SVU (middle right), DTL SVU (bottom left), MTL SVU (bottom right); color scale - cm

5. TOPOGRAPHY OF THE SEA SURFACE (TSS)

5.1 Generation of TSS field

Based on the VDatum transformation roadmap adopted for Chesapeake/Delaware Bay (shown in Figure 31), the topography of the sea surface (TSS) is defined as the elevation of the xGEOID20 B relative to Local Mean Sea Level (LMSL). xGEOID is a series of experimental geoid models published by the National Geodetic Survey (NGS) using satellite gravity models, terrestrial gravity and airborne gravity (https://beta.ngs.noaa.gov/GEOID/xGEOID/index.shtml). xGEOID is a preliminary product as NGS is progressing towards the final release of a newly updated national geopotential reference frame. Note that xGEOID20 B refers to one of xGEOID products that uses source data roughly available until 2020 and, B indicates this particular products use of the airborne gravity data that better captures smaller scale signals.

The TSS field for Chesapeake/Delaware Bay provides the spatial variations between a mean sea-level surface and the geopotential surface realized via xGEOID20 B. A positive value specifies that the xGEOID20 B reference value is further from the center of the Earth than the local mean sea-level surface.

For the Chesapeake/Delaware Bay TSS field, CO-OPS tide gauge and satellite altimetry datasets are used so that the majority of the development domain is available with long-term observations, as each dataset compensates another in their coverage.

A total of 95 tide stations have observed TSS values in this model domain. All mean sea level data are based on the most current National Tidal Datum Epoch (1983-2001). The observed TSS and their corresponding standard deviations are listed in the Appendix B. As all the tide gauges have tidal benchmark(s) that were GNSS campaigned to obtain ellipsoidal heights, all the tide gauge observations are referenced to the local mean sea level with regard to the IGS14 (a published reference frame from International GNSS Service) to which the xGeoid20B is referenced. Figure 32 shows the locations of tide stations with a color code for the observed TSS values and their corresponding standard deviations after all processing is applied. The observed TSS values in this model domain range from 0.165 m to 0.524 m. The observed TSS values in a few upstream gauges in the Delaware River and the James River are below 0.2 m. The standard deviation of the TSS values range from 0.022 m to 0.042 m, and is less than 0.035 m at most tide stations.

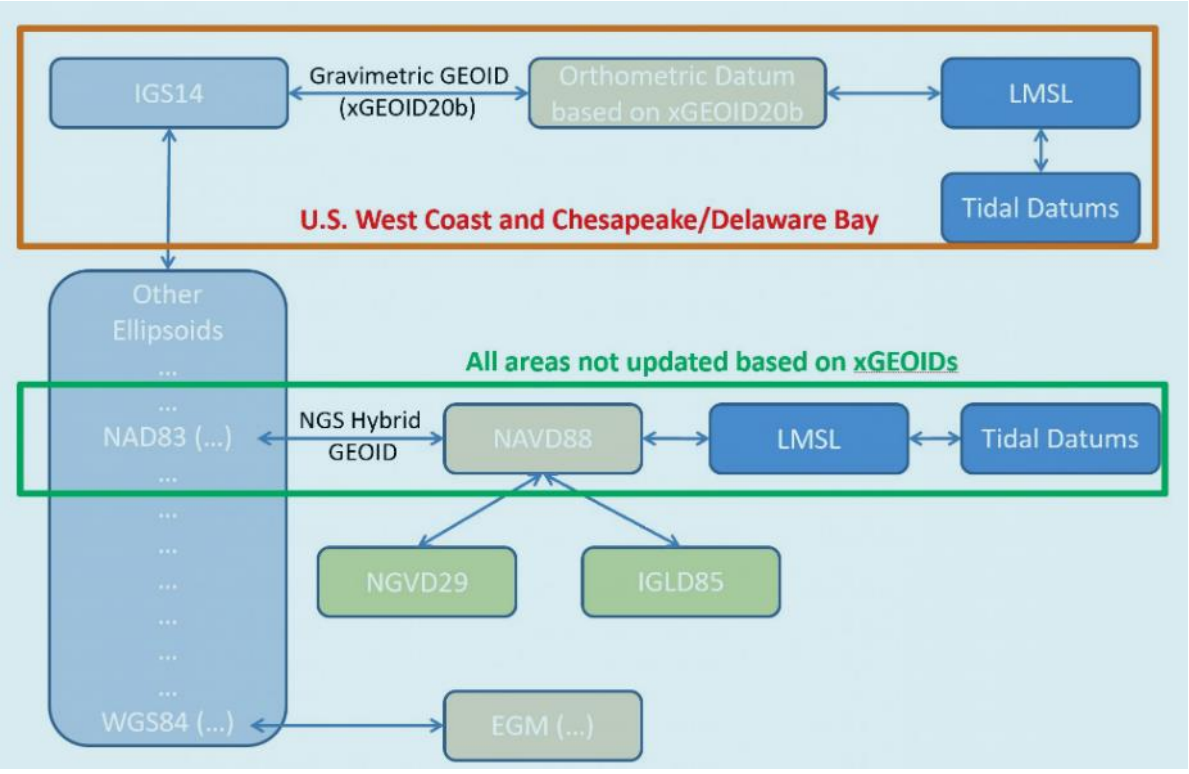

Figure 31. VDatum transformation roadmap adopted for Chesapeake/Delaware Bay

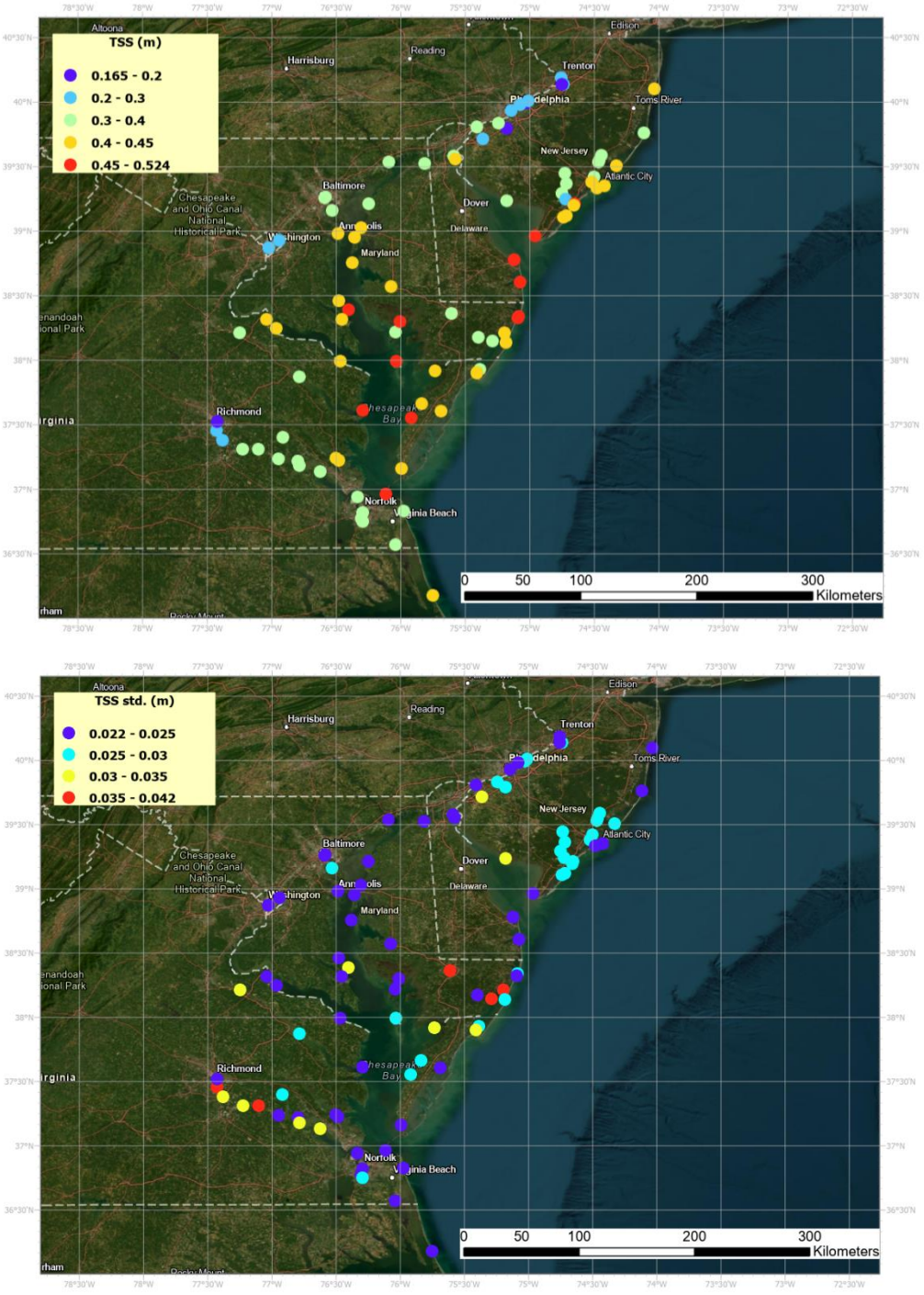

Figure 32. Locations of tide stations with the observed TSS values (top) and their corresponding standard deviations (bottom)

For about the last three decades, high precision satellite altimetry data has been accumulated for many oceanographic studies, among those 6 altimetry satellites and corresponding 8 missions (both repeat and geodetic) are chosen for the Chesapeake/Delaware Bay domain. Datasets are obtained from the Open Altimeter Database (OpenADB) and Radar Altimeter Database System (RADS). Details of these datasets are described in Table 6. Among the 8 missions, merged repeat tracks of Jason 1,2 and 3 are selected as the reference track to which other missions are referenced. Figure 33 illustrates the merged repeat tracks in the Chesapeake/Delaware Bay area, one from Jason-1, Jason-2 and Jason-3 (or the J123 track), and another from Envisat and Saral/Altika (or the N1SA track). Note that geodetic mission tracks are not drawn in the figure as these tracks cover the domain very densely.

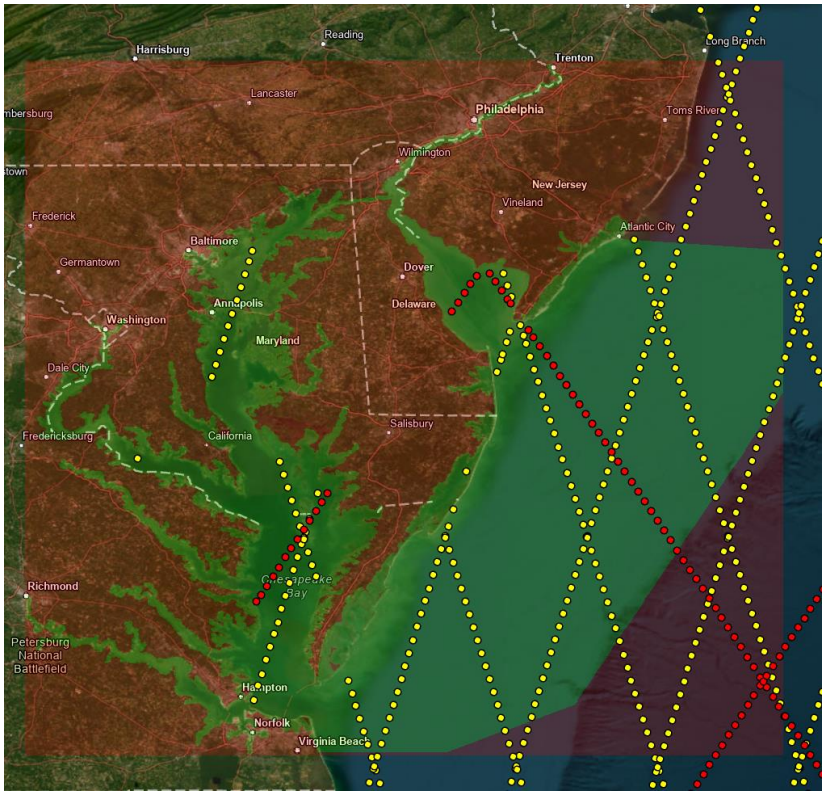

Figure 333. Illustration of merged repeat tracks in the Chesapeake/Delaware Bay area: J123 track (red dots) and N1SA track (yellow dots)

Original sea surface height (SSH) provided in the altimetry dataset is converted to be consistent with TSS values derived from tide gauges by considering i) the reference ellipsoid and ii) permanent tide. In general, altimetric SSH is not referenced to the GRS80 ellipsoid, that IGS14 reference frame uses as its reference ellipsoid. A reference ellipsoid conversion is applied (from TOPEX/Poseidon or T/P reference ellipsoid to GRS80 ellipsoid): for example, an original Jason-1 SSH (i.e. latitude, longitude and SSH referenced to the T/P ellipsoid) is transformed to geocentric coordinates (i.e. Earth centered cartesian coordinate). Then converted back to geographic coordinates referenced to the GRS80 ellipsoid. Here it is assumed that the T/P ellipsoid is defined fairly close to the earth's center similar to the IGS14 reference frame. Secondly, permanent tide conversion (from 'mean tide' to 'tide free') is applied. As the external tidal potential from the sun and moon consists of permanent (i.e. constant) and periodic (i.e. time-varying) components, handling of the permanent component and corresponding solid earth deformation differ by three permanent tide modes, i.e. mean tide, free tide and zero tide. Typically, as altimetric SSH only corrects for the time-varying periodic parts, SSH is regarded as the 'mean tide' quantity, but xGEOID is defined in the tide free system, which eliminates all the tidal effect. Thus, permanent tide conversion from mean tide to tide free is applied before deriving the TSS.

Table 6 Altimetry datasets used for the TSS field

Track	Mission	Cycle/Period
J1 repeat track	Jason-1 (J1)	001 - 259 (Jan 2002 - Jan 2009)
J2 repeat track	Jason-2 (J2)	001 - 303 (Jul 2008- Oct 2016)
J3 repeat track	Jason-3 (J3)	001 - 117 (Feb 2016- Apr 2019)
N1 repeat track	Envisat (N1)	007 - 093 (Jun 2002 - Oct 2010)
SA repeat track	SARAL/AltiKa (SA)	001 - 035 (Mar 2013- Jul 2016)
J1GM (~1 year)	Jason-1 (J1GM)	500 - 537 (May 2012- Jun 2013)
SAdp (~3 year)	SARAL/AltiKa drifting phase (SAdp)	100 - 128 (Jul 2016- Apr 2019)
C2 (~10 years)	Cryosat-2 (C2)	003 - 131 (Jul 2010- Jun 2020)

Once the basic conversion is done for all of the altimetry SSH datasets, integration processing of the multi-mission dataset (i.e. 8 missions in the domain) is applied. These steps include: i) determination of horizontal reference location of five repeat missions (i.e. Jason-1, Jason-2, Jason-3, Envisat, and Saral/Altika) using X-Track data (a regional altimetry data product for coastal areas produced by Center of Topography of the Ocean and the Hydrosphere in France), ii) mean SSH estimation along the determined repeat tracks with filtering based on SSH quality statistics, iii) repeat track SSH residual adjustment for cross-over points, iv) geodetic mission SSH track filtering based on SSH quality statistics, v) geodetic mission SSH residual adjustment using the reference tracks, vi) data thinning to merge repeat and geodetic mission SSHs using the stochastic information derived from the cross-over adjustments, and vii) vertical offset adjustment for the bias between altimetric and tide gauge TSS. After these steps, a consistent set of merged data points from altimetry and tide gauge is obtained.

The TSS field was derived by interpolating orthometric-to-MSL relationships which were obtained through the calculation of the xGEOID20 B-to-MSL values at derived data points. Breaklines were taken into consideration in the interpolation module when generating TSS field for representing the influence of land. A sea surface topography field was then generated using the Surfer© software's minimum curvature algorithm to create a surface that honors the data as closely as possible. The maximum allowed departure value used was 0.001 meters. To control the amount of bowing on the interior and at the edges of the grid, an internal and boundary tension of 0.3 was utilized. Once the gridded TSS field was generated for the entire domain (i.e. all VDatum sub-regions from R1 to R7 for the Chesapeake/Delaware Bay), the TSS field is exported to each sub-region based on marine grid extent. Null values were obtained from the tidal datum marine grids and were assigned to the sub-region TSS field as the null value locations represents the presence of land. Grid parameters for the TSS field are listed in Table 7.

Table 7 VDatum TSS grid parameters for the Chesapeake/Delaware Bay domain

VDatum Region	Longitude-Latitude Window	Zonal Spacing (deg)	Meridional Spacing (deg)	No. of Zonal Nodes	No. of Meridional Nodes
all sub regions	[36.729 40.250 -77.440 -73.593]	0.001	0.001	3848	3522

5.2 Generation of TSS SVU (spatially varying uncertainty) field

The tide gauge observation uncertainty values and estimated uncertainty for altimetry data are used to generate the TSS SVU field. Mean sea level observation uncertainties provided by CO-OPS, geoid uncertainty and ellipsoid height uncertainty from the GNSS campaign are further considered to obtain the TSS uncertainty at tide gauges. For altimetry datasets, uncertainties are estimated for both repeat and geodetic mission tracks considering the post cross-over adjustment statistic using the J123 track as a reference track. The cross-over adjustment based statistic is a consistent and realistic quantization of uncertainty for multi-mission altimetry dataset by mitigating bias between different altimetry missions. Then geoid uncertainty is further considered to obtain the TSS uncertainty at altimetry data points. Using these two uncertainty sources, SVU field is created by applying i) a rigorous error propagation approach that uses error sensitivity metric and full covariance matrix, and ii) a simple objective analysis that estimates the final TSS uncertainty given tide gauge observation and altimetry data uncertainties.

5.3 Interpolated TSS and TSS SVU results

The interpolated TSS field and the TSS SVU field are shown in Figure 34.

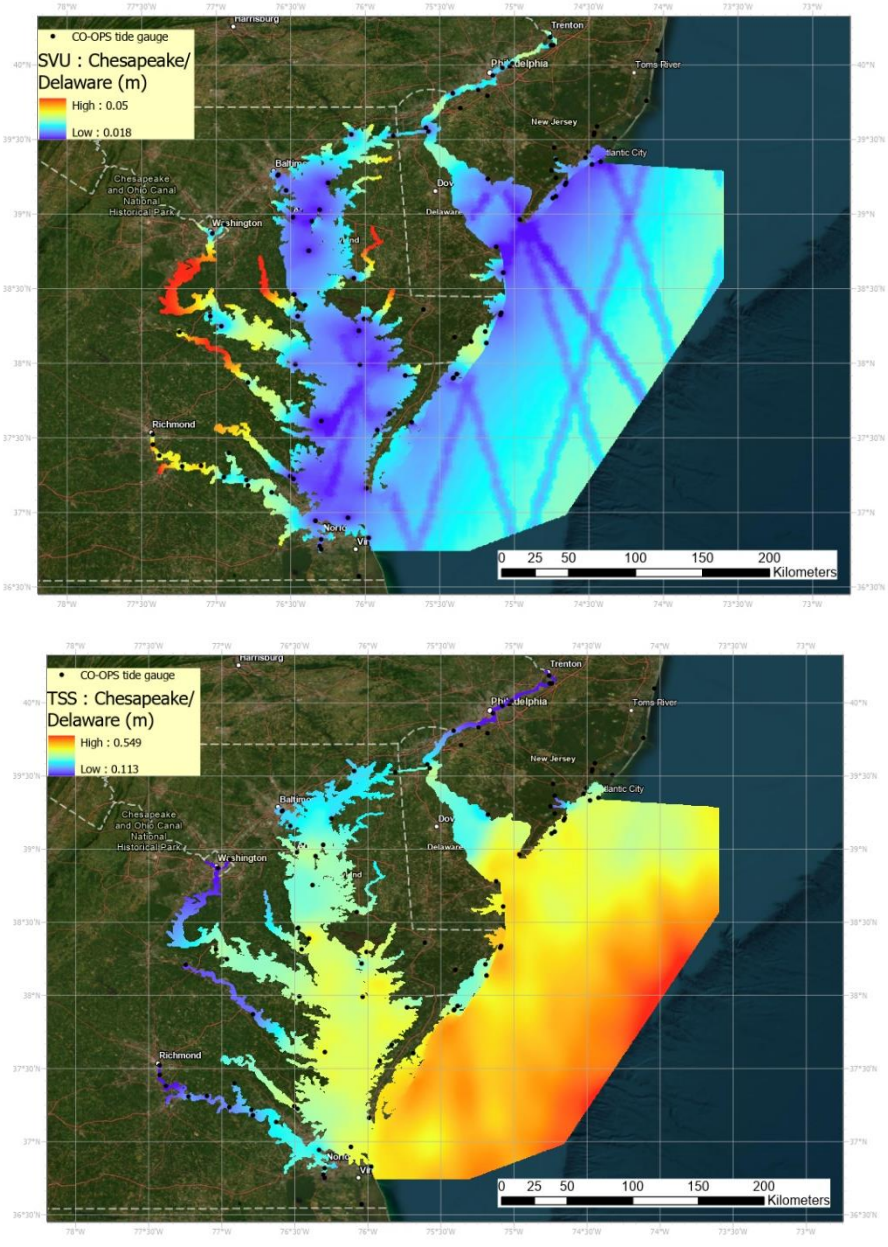

Figure 344. The interpolated TSS field (top) and the TSS SVU field (bottom) for the Chesapeake/Delaware Bay Regional Model

The statistical values of the interpolated TSS field and its SVU field are listed in Tables 8.

Table 8 Statistics of the interpolated TSS field and the TSS SVU field (in units of meters)

Region	Field	Minimum	Maximum	Mean	Standard Deviation
all sub regions	TSS	0.113	0.549	0.458	0.045
all sub regions	TSS Uncertainty	0.018	0.050	0.025	0.004

The tide gauge data used to compile TSS field grid was compared against the TSS grid product, to generalize internal consistency. The delta between TSS value for each tide station and the created TSS field grid is depicted in Table 9. Note that comparisons are made only for tide gauges inside the VDatum TSS model domain. Mean and standard deviation for these delta values are listed in Table 10.

Table 9 Tide station data utilized for TSS creation and deltas computed against the TSS grid

ID	Latitude (deg)	Longitude (deg)	NAVD 88 to MSL (m)	TSS Derived Value (m)	Delta (m)
8534657	-74.51830	39.38170	0.436	0.436	0.000
8534691	-74.71670	39.36830	0.317	0.317	0.000
8534770	-74.47670	39.33500	0.424	0.424	0.000
8535101	-74.64830	39.21500	0.507	0.506	0.001
8535163	-74.65670	39.20000	0.445	0.446	-0.001
8535375	-74.71670	39.12170	0.422	0.423	-0.001
8535419	-74.73830	39.11000	0.443	0.443	0.000
8536110	-74.95972	38.96778	0.524	0.523	0.001
8536931	-75.17500	39.23830	0.353	0.353	0.000
8539487	-74.73670	40.13670	0.208	0.208	0.000
8539993	-74.75500	40.18830	0.267	0.267	0.000
8540433	-75.40944	39.81167	0.340	0.340	0.000
8545240	-75.14167	39.93333	0.229	0.229	0.000
8546252	-75.07500	39.98333	0.272	0.272	0.000
8548989	-74.75189	40.13731	0.178	0.179	-0.001
8551762	-75.58830	39.58170	0.376	0.376	0.000
8551910	-75.57330	39.55830	0.439	0.438	0.001

8557380	-75.11916	38.78278	0.473	0.473	0.000
8558690	-75.07000	38.61000	0.465	0.465	0.000
8570255	-75.08500	38.34170	0.505	0.504	0.001
8570283	-75.09167	38.32833	0.478	0.479	-0.001
8570536	-75.19170	38.21500	0.409	0.409	0.000
8570649	-75.28500	38.14830	0.393	0.393	0.000
8571117	-76.03170	37.99500	0.460	0.460	0.000
8571421	-76.03867	38.22039	0.390	0.391	-0.001
8571559	-76.00500	38.30000	0.456	0.456	0.000
8571892	-76.07222	38.57417	0.416	0.416	0.000
8572271	-76.37500	38.75833	0.401	0.401	0.000
8572770	-76.35500	38.95670	0.416	0.416	0.000
8572955	-76.30170	39.03170	0.410	0.410	0.000
8573364	-76.24500	39.21333	0.358	0.358	0.000
8573927	-75.81000	39.52670	0.388	0.388	0.000
8574070	-76.09000	39.53670	0.367	0.367	0.000
8574680	-76.57833	39.26667	0.368	0.367	0.001
8574683	-76.58500	39.26170	0.357	0.357	0.000
8574931	-76.52670	39.16330	0.372	0.372	0.000
8575512	-76.48156	38.98328	0.427	0.427	0.000
8577004	-76.47330	38.46500	0.420	0.420	0.000
8577188	-76.39830	38.39170	0.483	0.483	0.000
8577330	-76.45083	38.31722	0.439	0.439	0.000
8579997	-76.93830	38.93330	0.237	0.237	0.000
8594900	-77.02167	38.87333	0.289	0.289	0.000
8630249	-75.38330	37.93170	0.398	0.398	0.000
8630308	-75.40500	37.90670	0.428	0.429	-0.001
8630316	-75.40670	37.90330	0.444	0.443	0.001
8632200	-75.98844	37.16519	0.428	0.428	0.000
8632869	-75.91670	37.55670	0.451	0.451	0.000
8633091	-75.83330	37.66670	0.424	0.424	0.000
8633777	-75.72830	37.92170	0.434	0.434	0.000
8635027	-77.03661	38.31975	0.424	0.424	0.000
8635150	-76.96000	38.25170	0.409	0.409	0.000
8635257	-77.24330	38.21330	0.313	0.313	0.000
8635750	-76.46461	37.99539	0.427	0.427	0.000
8635985	-76.78330	37.87330	0.324	0.324	0.000
8636580	-76.29000	37.61611	0.464	0.464	0.000

8636941	-77.42078	37.45956	0.210	0.210	0.000
8637624	-76.50000	37.24670	0.442	0.442	0.000
8637689	-76.47880	37.22650	0.415	0.415	0.000
8637712	-76.79142	37.22011	0.375	0.375	0.000
8638017	-76.62275	37.13822	0.389	0.389	0.000
8638433	-76.78330	37.18500	0.335	0.335	0.000
8638445	-76.91170	37.40330	0.358	0.358	0.000
8638450	-76.94330	37.24000	0.333	0.333	0.000
8638464	-77.09830	37.31500	0.324	0.324	0.000
8638476	-77.22330	37.31330	0.349	0.349	0.000
8638491	-77.37830	37.38330	0.293	0.293	0.000
8638495	-77.42000	37.52500	0.178	0.178	0.000
8638610	-76.33000	36.94667	0.377	0.377	0.000
8638660	-76.29330	36.82170	0.400	0.400	0.000
8638863	-76.11330	36.96670	0.451	0.451	0.000
8639207	-75.97330	36.83170	0.393	0.394	-0.001
8639348	-76.30169	36.77831	0.395	0.395	0.000
8639414	-76.29330	36.75500	0.311	0.311	0.000

Table 10 Mean and standard deviation of delta values tabulated in Table 9 (meters)

Region	Mean Delta Value (m)	Standard Deviation (m)
all sub regions	0.000003	0.0004

5.4 Summary

Finally, the TSS field and the TSS SVU field were created by the NGS by using i) observed TSS values (with regard to xGEOID product) and their corresponding uncertainties at 95 tide stations, and ii) ~19 years of multi mission satellite altimetry dataset, and their estimated uncertainties. The TSS field was created by interpolating orthometric-to-MSL relationships in tide gauges and altimetry dataset. The TSS SVU field was generated by applying a rigorous error propagation approach and a simple objective analysis.

ACKNOWLEDGMENTS

The authors thank Dr. Alexander Kuparov, Dr. Bahram Khazaei, and Dr. Lei Shi for reviewing this report and providing many helpful suggestions; Dr. Zizang Yang for overseen the preparation of the manuscript for production; and Dr. Edward Myers for management support over the course of the product development.
Special thanks to Lei Shi for supplying the VDatum team with Matlab scripts which implement the variational data assimilation technique for computing tidal datums and their uncertainties, following an approach suggested by Lei Shi and Edward Myers [2016].
Authors also thank the NOAA/CSDL' IT group, and the VDatum project tri-office management for their support of the project.

APPENDIX A

Table 11. CO-OPS tidal stations IDs and locations (decimal degree, longitude and latitude), tidal datums (meters) relative to local MSL, and r.m.s. error of observed datums as assigned by CO-OPS (cm), if available.

No	Station ID	lon, ^{o}W	lat, ^{o}N	MHHW, m	MHW, m	MLW, m	MLLW, m	r.m.s., cm
1	8533615	74.1117	39.7617	0.410	0.339	-0.318	-0.355	0.5
2	8534044	74.2628	39.6135	0.384	0.308	-0.294	-0.320	1.9
3	8534048	74.2100	39.6133	0.349	0.266	-0.284	-0.301	2.5
4	8534208	74.2567	39.5483	0.412	0.327	-0.328	-0.362	1.8
5	8534244	74.3867	39.5400	0.601	0.493	-0.477	-0.516	1.6
6	8534319	74.3250	39.5083	0.543	0.442	-0.430	-0.472	1.6
7	8534496	74.3633	39.4350	0.652	0.541	-0.564	-0.610	1.8
8	8534657	74.5183	39.3817	0.716	0.598	-0.610	-0.652	1.7
9	8534720	74.4183	39.3550	0.728	0.601	-0.623	-0.675	0.0
10	8534739	74.5400	39.3517	0.706	0.587	-0.608	-0.658	1.4
11	8534770	74.4767	39.3350	0.733	0.605	-0.625	-0.678	0.7
12	8534836	74.5333	39.3083	0.701	0.578	-0.574	-0.619	1.4
13	8535101	74.6483	39.2150	0.690	0.572	-0.585	-0.635	1.4
14	8535163	74.6567	39.2000	0.682	0.562	-0.597	-0.648	1.4
15	8535221	74.7100	39.1767	0.706	0.590	-0.612	-0.660	1.8
16	8535309	74.7500	39.1467	0.673	0.553	-0.571	-0.602	2.0
17	8535375	74.7167	39.1217	0.709	0.590	-0.616	-0.671	NaN
18	8535419	74.7383	39.1100	0.728	0.606	-0.627	-0.679	NaN
19	8535581	74.7650	39.0567	0.732	0.613	-0.664	-0.713	NaN
20	8535835	74.8233	38.9750	0.783	0.649	-0.664	-0.719	1.3
21	8536110	74.9600	38.9683	0.877	0.744	-0.734	-0.783	0.0

No	Station ID	lon, ^{o}W	lat, ^{o}N	MHHW, m	MHW, m	MLW, m	MLLW, m	r.m.s., cm
22	8536581	74.8917	39.1283	0.954	0.823	-0.905	-0.963	1.5
23	8536931	75.1750	39.2383	0.986	0.862	-0.922	-0.974	2.1
24	8537121	75.3750	39.3050	0.966	0.838	-0.878	-0.933	0.8
25	8538886	75.0430	40.0119	1.070	0.957	-1.052	-1.109	0.6
26	8539094	74.8697	40.0817	1.177	1.067	-1.158	-1.219	0.6
27	8539487	74.7367	40.1367	1.290	1.179	-1.230	-1.291	1.6
28	8539993	74.7550	40.1883	1.300	1.190	-1.302	-1.363	0.8
29	8540433	75.4100	39.8117	0.917	0.805	-0.900	-0.954	0.5
30	8545240	75.1417	39.9333	0.976	0.854	-1.005	-1.063	0.1
31	8545530	75.1383	39.9533	1.011	0.893	-1.010	-1.069	0.5
32	8546252	75.0750	39.9833	1.030	0.911	-1.036	-1.094	NaN
33	8548989	74.7517	40.1367	1.237	1.131	-1.259	-1.320	0.5
34	8551762	75.5883	39.5817	0.927	0.811	-0.847	-0.902	0.5
35	8551910	75.5733	39.5595	0.890	0.793	-0.835	-0.890	0.0
36	8554399	75.4000	39.1850	0.929	0.797	-0.827	-0.882	1.7
37	8555889	75.1130	38.9870	0.881	0.747	-0.747	-0.796	0.5
38	8557380	75.1200	38.7817	0.738	0.610	-0.631	-0.680	0.0
39	8558690	75.0700	38.6100	0.443	0.361	-0.405	-0.452	0.6
40	8570255	75.0850	38.3417	0.274	0.221	-0.244	-0.284	1.9
41	8570280	75.0833	38.3267	0.620	0.506	-0.519	-0.567	0.5
42	8570282	75.0900	38.3317	0.389	0.321	-0.349	-0.395	1.6
43	8570283	75.0917	38.3283	0.361	0.300	-0.341	-0.390	0.6
44	8570536	75.1917	38.2150	0.094	0.070	-0.073	-0.104	3.4
45	8570649	75.2850	38.1483	0.104	0.079	-0.082	-0.113	3.5

No	Station ID	lon, ^{o}W	lat, ^{o}N	MHHW, m	MHW, m	MLW, m	MLLW, m	r.m.s., cm
46	8571091	75.8633	37.9767	0.351	0.299	-0.268	-0.305	1.9
47	8571117	76.0317	37.9950	0.277	0.223	-0.241	-0.287	1.6
48	8571421	76.0387	38.2204	0.314	0.265	-0.271	-0.311	0.6
49	8571559	76.0050	38.3000	0.372	0.320	-0.317	-0.357	1.0
50	8571579	76.2650	38.3417	0.232	0.180	-0.192	-0.241	1.2
51	8571773	75.8183	38.4833	0.341	0.296	-0.354	-0.408	0.8
52	8571892	76.0617	38.5725	0.311	0.247	-0.247	-0.311	0.0
53	8572271	76.3750	38.7583	0.232	0.165	-0.171	-0.238	0.8
54	8572467	76.3733	38.8367	0.238	0.168	-0.171	-0.235	0.7
55	8572669	75.9450	38.9167	0.360	0.308	-0.390	-0.445	2.2
56	8572770	76.3550	38.9567	0.226	0.149	-0.162	-0.226	0.7
57	8572955	76.3017	39.0317	0.265	0.177	-0.183	-0.250	0.7
58	8573349	75.9250	39.2450	0.421	0.329	-0.344	-0.421	1.1
59	8573364	76.2450	39.2133	0.274	0.180	-0.189	-0.253	0.1
60	8573704	76.0633	39.3717	0.344	0.241	-0.247	-0.314	1.6
61	8573903	75.9167	39.5033	0.433	0.338	-0.326	-0.384	0.8
62	8573927	75.8100	39.5285	0.503	0.445	-0.408	-0.475	0.5
63	8574070	76.0900	39.5367	0.384	0.280	-0.296	-0.360	0.3
64	8574459	76.2550	39.3883	0.277	0.171	-0.210	-0.268	1.9
65	8574680	76.5794	39.2669	0.259	0.171	-0.180	-0.247	0.0
66	8574683	76.5850	39.2617	0.262	0.171	-0.177	-0.244	1.0
67	8574821	76.5333	39.2083	0.274	0.177	-0.186	-0.250	1.3
68	8574931	76.5267	39.1633	0.253	0.162	-0.168	-0.232	1.4
69	8575109	76.4450	39.1000	0.232	0.146	-0.155	-0.223	1.8

No	Station ID	lon, ^{o}W	lat, ^{o}N	MHHW, m	MHW, m	MLW, m	MLLW, m	r.m.s., cm
70	8575512	76.4816	38.9833	0.216	0.143	-0.152	-0.219	0.0
71	8577004	76.4733	38.4650	0.201	0.152	-0.155	-0.207	0.8
72	8577188	76.3983	38.3917	0.229	0.152	-0.165	-0.192	2.5
73	8577330	76.4508	38.3172	0.219	0.174	-0.183	-0.232	0.0
74	8579542	76.6833	38.6550	0.311	0.268	-0.287	-0.338	0.8
75	8579997	76.9383	38.9333	0.524	0.454	-0.445	-0.497	1.2
76	8593005	76.9950	38.8717	0.503	0.430	-0.427	-0.475	1.1
77	8593909	76.9550	38.9100	0.530	0.460	-0.436	-0.479	1.3
78	8594900	77.0217	38.8730	0.494	0.424	-0.427	-0.472	0.0
79	8630111	75.3017	37.9817	0.140	0.116	-0.116	-0.146	3.1
80	8630249	75.3833	37.9317	0.290	0.241	-0.241	-0.271	1.8
81	8630308	75.4050	37.9067	0.399	0.332	-0.326	-0.357	2.3
82	8630316	75.4067	37.9033	0.445	0.372	-0.369	-0.411	2.5
83	8631542	75.7783	37.3017	0.719	0.619	-0.600	-0.649	1.0
84	8631935	75.5473	37.0878	0.637	0.549	-0.564	-0.591	NaN
85	8632085	75.9833	37.0967	0.503	0.427	-0.466	-0.512	1.4
86	8632200	75.9884	37.1652	0.463	0.393	-0.399	-0.436	0.0
87	8632837	76.0150	37.5383	0.283	0.232	-0.247	-0.287	1.8
88	8632869	75.9167	37.5567	0.311	0.259	-0.268	-0.314	1.9
89	8633091	75.8333	37.6667	0.317	0.262	-0.274	-0.305	1.7
90	8633362	75.7733	37.7633	0.347	0.296	-0.296	-0.341	2.9
91	8633532	75.9933	37.8283	0.277	0.229	-0.232	-0.259	2.2
92	8633777	75.7283	37.9217	0.393	0.341	-0.338	-0.381	2.3
93	8635027	77.0366	38.3197	0.290	0.238	-0.241	-0.287	NaN

No	Station ID	lon, ^{o}W	lat, ^{o}N	MHHW, m	MHW, m	MLW, m	MLLW, m	r.m.s., cm
94	8635150	76.9600	38.2517	0.296	0.247	-0.250	-0.296	0.0
95	8635257	77.2433	38.2133	0.347	0.299	-0.351	-0.393	2.4
96	8635750	76.4647	37.9953	0.229	0.186	-0.195	-0.232	0.0
97	8635985	76.7833	37.8733	0.305	0.259	-0.287	-0.323	1.9
98	8636580	76.2900	37.6161	0.213	0.171	-0.180	-0.210	0.7
99	8636653	76.9900	37.5833	0.479	0.427	-0.494	-0.527	3.2
100	8636941	77.4208	37.4596	0.500	0.424	-0.503	-0.546	3.2
101	8637624	76.5000	37.2467	0.427	0.366	-0.360	-0.393	0.0
102	8637689	76.4788	37.2265	0.408	0.347	-0.341	-0.378	0.6
103	8637712	76.7914	37.2201	0.326	0.274	-0.280	-0.329	2.6
104	8638017	76.6227	37.1382	0.381	0.326	-0.341	-0.390	2.0
105	8638339	76.3991	36.8232	0.481	0.417	-0.426	-0.470	1.3
106	8638424	76.6633	37.2200	0.408	0.344	-0.344	-0.390	2.2
107	8638433	76.7833	37.1850	0.357	0.296	-0.299	-0.351	2.6
108	8638445	76.9117	37.4033	0.418	0.369	-0.411	-0.448	1.7
109	8638449	76.9483	37.2317	0.314	0.256	-0.287	-0.332	0.9
110	8638450	76.9433	37.2400	0.329	0.268	-0.302	-0.344	0.9
111	8638464	77.0983	37.3150	0.372	0.299	-0.347	-0.396	3.2
112	8638476	77.2233	37.3133	0.418	0.338	-0.381	-0.415	2.5
113	8638481	77.2700	37.3133	0.430	0.354	-0.396	-0.430	2.4
114	8638489	77.3717	37.2667	0.442	0.375	-0.475	-0.524	4.0
115	8638491	77.3783	37.3833	0.491	0.415	-0.463	-0.500	2.4
116	8638495	77.4200	37.5250	0.536	0.469	-0.539	-0.585	1.0
117	8638610	76.3300	36.9467	0.427	0.366	-0.375	-0.415	0.0

No	Station ID	lon, ^{o}W	lat, ^{o}N	MHHW, m	MHW, m	MLW, m	MLLW, m	r.m.s., cm
118	8638660	76.2933	36.8217	0.482	0.418	-0.422	-0.464	0.6
119	8638863	76.1133	36.9667	0.453	0.383	-0.394	-0.431	0.0
120	8638901	76.0833	37.0329	0.472	0.396	-0.411	-0.451	NaN
121	8638999	76.0067	36.9300	0.547	0.469	-0.481	-0.519	1.5
122	8639208	75.9683	36.8317	0.573	0.487	-0.514	-0.551	2.3
123	8639348	76.3017	36.7783	0.499	0.435	-0.437	-0.478	0.3
124	8639414	76.2933	36.7550	0.509	0.443	-0.446	-0.491	1.3
125	8639428	75.9200	36.6917	0.597	0.506	-0.518	-0.570	1.9
126	8651370	75.7615	36.2150	0.585	0.487	-0.495	-0.539	0.0
127	8570691	75.2000	38.1389	0.125	0.094	-0.091	-0.125	NaN
128	8535055	75.0328	39.2325	0.957	0.826	-0.896	-0.954	NaN
129	8538875	75.0083	40.0133	1.065	0.959	-0.988	-1.020	1.6
130	8639219	75.9817	36.8250	0.613	0.510	-0.523	-0.569	1.8
131	8639214	75.9750	36.8250	0.604	0.501	-0.513	-0.557	1.8
132	8639207	75.9733	36.8317	0.584	0.496	-0.507	-0.547	0.9
133	8639208	75.9683	36.8317	0.573	0.487	-0.514	-0.551	2.3
134	8534883	74.7483	39.2950	0.587	0.499	-0.509	-0.548	0.1
135	8534691	74.7167	39.3800	0.588	0.499	-0.509	-0.548	0.1
136	8631591	75.9250	37.2883	0.587	0.498	-0.509	-0.547	0.1

APPENDIX B

Tide station data utilized for TSS creation and their corresponding uncertainty in terms of standard deviations

ID	Latitude (deg)	Longitude (deg)	TSS (m)	Uncertainty (m)
8532591	-74.03500	40.10170	0.406	0.024
8533615	-74.11170	39.76170	0.385	0.023
8534104	-74.44170	39.59170	0.362	0.028
8534212	-74.46170	39.54830	0.349	0.028
8534256	-74.46330	39.53500	0.353	0.028
8534319	-74.32500	39.50830	0.415	0.026
8534468	-74.72830	39.44830	0.341	0.027
8534540	-74.50000	39.42330	0.396	0.027
8534657	-74.51830	39.38170	0.436	0.028
8534691	-74.71670	39.36830	0.317	0.029
8534720	-74.41830	39.35500	0.440	0.022
8534770	-74.47670	39.33500	0.424	0.023
8534883	-74.74830	39.29500	0.324	0.029
8535001	-74.71830	39.24670	0.293	0.030
8535101	-74.64830	39.21500	0.507	0.026
8535163	-74.65670	39.20000	0.445	0.026
8535375	-74.71670	39.12170	0.422	0.026
8535419	-74.73830	39.11000	0.443	0.026
8536110	-74.95972	38.96778	0.524	0.022
8536931	-75.17500	39.23830	0.353	0.031
8538274	-75.36000	39.71500	0.253	0.032
8538438	-75.17670	39.79500	0.165	0.028
8538512	-75.23830	39.83500	0.345	0.026
8538853	-75.02830	39.99330	0.168	0.026
8538875	-75.00830	40.01330	0.232	0.027
8539487	-74.73670	40.13670	0.208	0.027
8539993	-74.75500	40.18830	0.267	0.024
8540433	-75.40944	39.81167	0.340	0.023
8545240	-75.14167	39.93333	0.229	0.022
8546252	-75.07500	39.98333	0.272	0.024

8548989	-74.75189	40.13731	0.178	0.022
8551762	-75.58830	39.58170	0.376	0.022
8551910	-75.57330	39.55830	0.439	0.022
8557380	-75.11916	38.78278	0.473	0.022
8558690	-75.07000	38.61000	0.465	0.023
8570255	-75.08500	38.34170	0.505	0.029
8570283	-75.09167	38.32833	0.478	0.023
8570536	-75.19170	38.21500	0.409	0.041
8570649	-75.28500	38.14830	0.393	0.042
8570691	-75.18353	38.13894	0.449	0.026
8571117	-76.03170	37.99500	0.460	0.027
8571359	-75.39667	38.17833	0.361	0.023
8571421	-76.03867	38.22039	0.390	0.023
8571559	-76.00500	38.30000	0.456	0.024
8571616	-75.60670	38.36500	0.364	0.037
8571892	-76.07222	38.57417	0.416	0.022
8572271	-76.37500	38.75833	0.401	0.024
8572770	-76.35500	38.95670	0.416	0.023
8572955	-76.30170	39.03170	0.410	0.023
8573364	-76.24500	39.21333	0.358	0.022
8573927	-75.81000	39.52670	0.388	0.022
8574070	-76.09000	39.53670	0.367	0.023
8574680	-76.57833	39.26667	0.368	0.022
8574683	-76.58500	39.26170	0.357	0.024
8574931	-76.52670	39.16330	0.372	0.026
8575512	-76.48156	38.98328	0.427	0.022
8577004	-76.47330	38.46500	0.420	0.024
8577188	-76.39830	38.39170	0.483	0.034
8577330	-76.45083	38.31722	0.439	0.022
8579997	-76.93830	38.93330	0.237	0.025
8594900	-77.02167	38.87333	0.289	0.022
8630249	-75.38330	37.93170	0.398	0.029
8630308	-75.40500	37.90670	0.428	0.032
8630316	-75.40670	37.90330	0.444	0.034
8631044	-75.68583	37.60778	0.449	0.022
8632200	-75.98844	37.16519	0.428	0.022
8632869	-75.91670	37.55670	0.451	0.029
8633091	-75.83330	37.66670	0.424	0.028

8633777	-75.72830	37.92170	0.434	0.032
8635027	-77.03661	38.31975	0.424	0.024
8635150	-76.96000	38.25170	0.409	0.022
8635257	-77.24330	38.21330	0.313	0.033
8635750	-76.46461	37.99539	0.427	0.022
8635985	-76.78330	37.87330	0.324	0.029
8636580	-76.29000	37.61611	0.464	0.023
8636941	-77.42078	37.45956	0.210	0.039
8637624	-76.50000	37.24670	0.442	0.022
8637689	-76.47880	37.22650	0.415	0.022
8637712	-76.79142	37.22011	0.375	0.024
8638017	-76.62275	37.13822	0.389	0.031
8638433	-76.78330	37.18500	0.335	0.034
8638445	-76.91170	37.40330	0.358	0.028
8638450	-76.94330	37.24000	0.333	0.024
8638464	-77.09830	37.31500	0.324	0.039
8638476	-77.22330	37.31330	0.349	0.034
8638491	-77.37830	37.38330	0.293	0.033
8638495	-77.42000	37.52500	0.178	0.024
8638610	-76.33000	36.94667	0.377	0.022
8638660	-76.29330	36.82170	0.400	0.023
8638863	-76.11330	36.96670	0.451	0.022
8639207	-75.97330	36.83170	0.393	0.024
8639348	-76.30169	36.77831	0.395	0.022
8639414	-76.29330	36.75500	0.311	0.026
8639908	-76.03830	36.57670	0.327	0.022
8651370	-75.74669	36.18331	0.433	0.022

REFERENCES

Hess, K. W., 2002: Spatial interpolation of tidal data in irregularly-shaped coastal regions by numerical solution of Laplace's equation. Estuarine, Coastal and Shelf Science, 54(2), 175-192.

Hess, K. W., 2003: Water level simulation in bays by spatial interpolation of tidal constituents, residual water levels, and datums. Continental Shelf Research, 23(5), 395-414.

Szpilka, C.; Dresback, K.; Kolar, R.; Feyen, J.; Wang, J. Improvements for the Western North Atlantic, Caribbean and Gulf of Mexico ADCIRC Tidal Database (EC2015). J. Mar. Sci. Eng. 2016, 4, 72. https://doi.org/10.3390/jmse4040072

Milbert, D. G. and K. W. Hess, 2001: Combination of Topography and Bathymetry through Application of Calibrated Vertical Datum Transformations in the Tampa Bay Region. Proceedings of the 2nd Biennial Coastal GeoTools Conferences, Charleston, SC.

Shi, L. and E. Myers, 2016: Statistical Interpolation of Tidal Datums and Computation of Its Associated Spatially Varying Uncertainty. Journal of Marine Science and Engineering, 4, 1-11.

Yang, Z., E. Myers, A. Wong, and S. White, 2008: Vdatum for Chesapeake Bay, Delaware Bay, and Adjacent Coastal Water Areas: Tidal Datums and Sea surface Topography. U.S. Department of Commerce, National Oceanic and Atmospheric Administration, Silver Spring, Maryland, /NOAA Technical Memorandum /NOS CS 15, 110 pp.

Westerink, J.J., R.A. Luettich, Jr. and N.W. Scheffner, 1993, ADCIRC: an advanced three-dimensional circulation model for shelves coasts and estuaries, report 3: development of a tidal constituent data base for the Western North Atlantic and Gulf of Mexico, Dredging Research Program Technical Report DRP-92-6, U.S. Army Engineers waterways Experiment Station, Vicksburg, MS, 154p.

R.A. Luettich and J.J. Westerink, 2004. Formulation and Numerical Implementation of the 2D/3D ADCIRC Finite Element Model Version 44.XX https://adcirc.org/wp-content/uploads/sites/2255/2018/11/adcirc_theory_2004_12_08.pdf